# LANTHANIDE OXYCARBIDES: PHASE AND EQUILIBRIUM STUDIES

Thesis for the Degree of Ph. D.
MICHIGAN STATE UNIVERSITY
A. DUANE BUTHERUS
1969



#### This is to certify that the

thesis entitled

LANTHANIDE OXYCARBIDES: PHASE AND EQUILIBRIUM STUDIES

presented by

A. DUANE BUTHERUS

has been accepted towards fulfillment of the requirements for

Ph.D. degree in Chemistry

Major professor

Date August 6, 1969

#### ABSTRACT

# LANTHANIDE OXYCARBIDES: PHASE AND EQUILIBRIUM STUDIES

bу

#### A. Duane Butherus

#### Introduction

Oxycarbide phases of uranium have been reported by several workers. A report from this laboratory, however, first showed the existence of a ternary oxycarbide phase in a lanthanide system. In this thesis, studies on two distinctly different  $\text{Ln}(0,\mathbb{C})$  phases (Ln=lanthanide) will be reported in detail. The  $\text{Ln}_2\text{O}_2\text{C}_2$  phase has been prepared only for Ln=Nd, La. The  $\text{Ln}_4\text{O}_3\text{C}$  phase appears more general and has been prepared for Ln=La, Nd, Gd, Ho, Er. The  $\text{Ln}_2\text{O}_2\text{C}_2$  system has been studied quite thoroughly thermodynamically, though less so structurally. The  $\text{Ln}_4\text{O}_3\text{C}$  system on the other hand has been more thoroughly studied structurally.

#### Techniques

Preparative methods included induction heating in various crucibles and in sealed bombs, arc melting, electron-beam zone refining and arc zone refining. Preparative techniques were developed with the aid of phase purity studies, accomplished via X-ray powder diffraction methods and micrography.

Thermodynamic studies were effected through static methods, by utilizing induction heating to maintain sample temperatures. Carbon monoxide, the only gaseous component in the equilibrium system described by the equation

$$Ln_2O_3(s) + 3C(s) = Ln_2O_2C_2(s) + CO(g),$$
 (1)

exhibited an equilibrium pressure in the range of 1 to 150 torr for reaction temperatures of 1350° to 1850°. Both second- and third-law procedures of data reduction were employed.

Analytical procedures included gravimetric analysis for the metal, combustion for carbon, and vacuum fusion for oxygen. Structural studies utilized X-ray powder diffractometry.

## Results of Study

The equilibrium system described by equation (1) gave the following thermodynamic data:

$$\Delta H_{298}^{\circ}$$
 (Ln = Nd) =  $75 \cdot_9 \pm 3 \cdot_0 \text{kcal/gfw}$   
 $\Delta H_{298}^{\circ}$  (Ln = La) =  $82 \cdot_2 \pm 1 \cdot_9 \text{kcal/gfw}$   
 $\Delta S_{298}^{\circ}$  (Ln = Nd) =  $33 \cdot_3 \pm 4 \cdot_4 \text{eu/gfw}$   
 $\Delta S_{298}^{\circ}$  (Ln = La) =  $37 \cdot_7 \pm 3 \cdot_6 \text{eu/gfw}$ 

The standard enthalpies of formation at 298° are computed to be

$$\Delta H_{f}^{\circ} (Nd_{2}O_{2}C_{2}(s)) = -329._{8} \pm 3 \text{ kcal/}_{gfw},$$

$$\Delta H_{f}^{\circ} (La_{2}O_{2}C_{2}(s)) = -320._{0} \pm 2 \text{ kcal/}_{gfw};$$

and the standard free energies of formation at 298° are

$$\Delta G_{\mathbf{f}}^{\circ}$$
 (Nd<sub>2</sub>O<sub>2</sub>C<sub>2</sub>(s)) = -309·<sub>9</sub> ± 3·<sub>9</sub> kcal/gfw  
 $\Delta G_{\mathbf{f}}^{\circ}$  (La<sub>2</sub>O<sub>2</sub>C<sub>2</sub>(s)) = -315·<sub>6</sub> ± 2·<sub>9</sub> kcal/gfw.

The  $\mathrm{Nd}_4\mathrm{O}_3\mathrm{C}$  phase is shown to possess a NaCl-type fcc structure having a lattice parameter  $\mathrm{a}_0 = 5.1406 \pm 0.0007 \mathrm{\AA}$ , and appears to have oxide and methanide ions distributed randomly in the anionic lattice sites.

# LANTHANIDE OXYCARBIDES: PHASE AND EQUILIBRIUM STUDIES

by  $A^{(i)}_{\bullet}$  Duane Butherus

#### A Thesis

Submitted to
Michigan State University
in partial fulfillment of the requirements
for the degree of

DOCTOR OF PHILOSOPHY

Department of Chemistry 1969

#### ACKNOWLEDGMENTS

2 6 ' 6 2 ' )

My appreciation goes first to Dr. Harry Eick, whose wisdom, tolerance, guidance and patience made this work possible. Much invaluable help was also extended by John Haschke, whose discussions concerning some of the work were a great aid. The support of the U. S. Atomic Energy Commission (Contract AT(11-1)-716) is also gratefully acknowledged. Finally my most grateful thanks to my wife without whose patience and understanding this work would not have been started.

## TABLE OF CONTENTS

		page
Abstract Acknowledge Table of Collist of Tai List of Fi List of App	ontents bles gures	ii iii vi vii viii
Chapter I,	General Introduction	1
Chapter II	, La <sub>2</sub> O <sub>2</sub> C <sub>2</sub> Phase	4
Α.	Introduction, La <sub>2</sub> 0 <sub>2</sub> C <sub>2</sub>	4
В.	Theoretical Considerations  1. Thermodynamics  a. Relationships from the second law of thermodynamics  b. Heat Capacity Effects  c. Relationships from the third law of thermodynamics  2. Instrumental Theory  a. Optical Pyrometry  b. Absorption Corrections in Pyrometry  c. Two-Color Pyrometry	6 6 7 9 12 14 14 16 17
C.	Experimental Methods, Ln <sub>2</sub> O <sub>2</sub> C <sub>2</sub> 1. Synthesis  a. Starting materials  b. General techniques  c. Containers  d. Synthesis I  e. Synthesis II  f. Synthesis III  g. Synthesis IV  h. Synthesis V  2. Phase Purity  3. Analytical Procedures  a. Metal Analysis  b. Total Carbon Analysis  c. Hydrolysis Experiments  d. X-Ray Investigations  e. Infrared Studies  f. Equilibrium Studies	19 19 19 24 25 29 33 34 37 34 42 43 43

## Table of Contents (cont.)

		page
D.	Results of Ln <sub>2</sub> O <sub>2</sub> C <sub>2</sub> Investigations 1. Preparative Results 2. Analytical Results 3. Hydrolysis Results 4. X-Ray Diffraction Results 5. Infrared Results 6. Equilibrium Results	47 47 49 51 52 55
Ε.	<pre>Ln<sub>2</sub>0<sub>2</sub>C<sub>2</sub>, Conclusions and Discussion 1. General Discussion a. Stoichiometry and Bonding b. Structure</pre>	68 68 68 71
	2. Relationship of Lanthanum and Neodymium Analogues of Ln <sub>2</sub> O <sub>2</sub> C <sub>2</sub> a. Structure b. Thermodynamis 3. Phase Relationships	73 73 74 76
Chapter II	II, The Ln <sub>4</sub> 0 <sub>3</sub> C Phase	77
Α.	Introduction	77
В.	Experimental Methods 1. Preparation 2. Analysis a. Metal Analysis b. Carbon Analysis c. Oxygen Analysis d. X-Ray Analysis	78 78 84 84 85 87 92
C. D.	3. Hydrolysis Experiments 4. Equilibrium Studies Results, Ln <sub>4</sub> O <sub>3</sub> C 1. Preparatory Results 2. Analytical Results 3. X-Ray Analysis Results 4. Hydrolysis Results Discussion Ln <sub>4</sub> O <sub>3</sub> C Phase	92 93 94 95 95 99 100
	, Future Research	110
Α.	Ln <sub>2</sub> 0 <sub>2</sub> C <sub>2</sub> Phase	110
В.	1. Structure Determination 2. Bonding Studies Ln <sub>4</sub> 0 <sub>3</sub> C Phase	110 110 112
	<ol> <li>Structure and Bonding</li> <li>Thermodynamics</li> </ol>	112 112
	<ol><li>Proposed New Phases, Based on Chapter III</li></ol>	112

## Table of Contents (cont.)

	page
Chapter V, Bibliography	114
Chapter VI, Appendices	118

## LIST OF TABLES

Table I:	Observed Nd <sub>2</sub> O <sub>2</sub> C <sub>2</sub> X-Ray Powder Diffraction	
	Data pag	;e 53
Table II:	Observed La <sub>2</sub> O <sub>2</sub> C <sub>2</sub> X-Ray Powder Diffraction	
	Data pag	;e 54
Table III:	Calculated and Observed Diffraction	
	Itensities for (111) and (002)	
	Planes for Nd <sub>4</sub> O <sub>3</sub> C pag	e 100;

## LIST OF FIGURES

Figure 1.	Arc Melter	page	30
Figure 2.	Combustion Apparatus	page	40
Figure 3.	Double-Walled Graphite Crucible	page	59
Figure 4.	Pressure of Carbon Monoxide in		
	Equilibrium with Nd <sub>2</sub> O <sub>2</sub> C <sub>2</sub>	page	60
Figure 5.	Pressure of Carbon Monoxide in		
	Equilibrium with La <sub>2</sub> O <sub>2</sub> C <sub>2</sub>	page	61
Figure 6.	Oxygen Analysis System	page	88
Figure 7.	Pressure Measuring System	page	120
Figure 8.	Arc Zone Melter	page	122
Figure 9.	Electron-Beam Zone Melter	page	124

## LIST OF APPENDICES

Appendix I:	Source and Purity of Materialspage	118
Appendix II:	High-Speed Pumping System and	
	Current Concentratorpage	119
Appendix III:	Tentative Indexing of La <sub>2</sub> 0 <sub>2</sub> C <sub>2</sub> page	121
Appendix IV:	Arc Zone Melterpage	122
Appendix V:	Electron-Beam Zone Melterpage	123
Appendix VI:	Calculated Intensities of	
	Diffraction Lines for Nd403C in	
	ZnS- and NaCl-Type Latticespage	125
Appendix VII:	Effective Anionic Radiipage	126

#### CHAPTER I. GENERAL INTRODUCTION

# A. <u>Literature Concerning Lanthanide Oxides, Carbides,</u> and Oxycarbides

Since the original discovery of a lanthanide compound (Arrhenius, 1788, described by B. R. Geijer<sup>1</sup>), most of the chemistry of the lanthanide elements has involved the oxide system or compounds easily derived from the oxides by classical solution techniques. Such compounds as nitrates, oxalates, carbonates and sulfates, were used in the early separation techniques.<sup>2</sup>

Carbides of the lanthanides were first reported by Pettersson, who described the preparation of the dicarbides of La, Y, and Ce. The preparation was effected by melting together a mixture of the oxide and carbon in a high current electric arc. The formulas reported, based on analytical work, were YC<sub>1.87</sub> and LaC<sub>1.85</sub>. Pettersson was probably trying to reduce the oxides to form the metals, and it is possible that the samples contained considerable quantities of oxygen. Moissan et al. 4,5,6 prepared and reported hydrolytic studies on the lanthanum, neodymium and praseodymium dicarbides. Only within the past decade, however, have questions been raised as to the possibility of forming ternary metal-oxygen-carbon phases.

#### B. Carbides as Pseudo-Oxides

In the first approximation, new ionic solids of a given metallic element can be thought of as being formed from known compounds by exchanging the anions present for different ones. Thus the halides of the lanthanides may be thought of as being formed by substituting two halide ions for each oxide ion in the sesquioxide represented by the formula  $\text{LnO}_{1.5}$ . In the case of the carbides, the substitution may be considered as the replacement of an oxide ion  $\text{O}^{=}$  by an acetylide ion  $\text{C}_{2}^{=}$  accompanied by partial reduction of the metal.

Partial replacement of one type of anion by another is well known in the lanthanide-oxygen-halogen systems. The oxyhalides, LnOX, for example, may be considered a replacement of an oxide ion by two halogen ions in the formula 1/2 Ln<sub>2</sub>0<sub>3</sub>. This thesis proposes that a similar model of partial replacement of anions describes that lanthanide-oxygen-carbon system with carbide units replacing a fraction of the oxide units in the lanthanide oxide. By this model, carbide ions may be considered to be pseudo oxides.

### C. Purpose of this Research

This thesis reports the further elucidation of the work of  ${\tt G.}$  L Buchel,  ${\tt 7}$  which proposed the existence

of ternary lanthanide-oxygen-carbon systems, and the description of other phases discovered in the Ln(0,C) ternary systems.

## CHAPTER II. THE Ln202C2 PHASE

## A. INTRODUCTION, Ln<sub>2</sub>O<sub>2</sub>C<sub>2</sub>

Equilibrium systems of the general type

$$MO_{\mathbf{x}}(s) + (x+y)C(s) = MC_{\mathbf{y}}(s) + xCO(g)$$
 (1)

have been studied by a numer of workers for the phases formed when  $M = uranium.^{8-11}$  As early as 1925, Otto Heusler, busing a vacuum furnace, reported equilibrium data over the temperature range of 1480° to 1801° for the above reaction when x and y both equal 2. Further research into the uranium-carbon system, however, disclosed the possible presence of other uranium-carbon phases in this temperature range. The existence of the monocarbide up to temperatures of 1800° was confirmed in 1948, 12 and the existence of the sesquicarbide was confirmed, but there is some doubt about the temperature range over which it exists. 13 In addition, several crystal modifications of the phases may be present. Complicating the uranium-carbon system even more is the existence of uranium-carbon-oxygen solid tenary phases which may also be in equilibrium with carbon monoxide. 10,14,15 of these complications, most current thermodynamic investigations in this system are accomplished by vaporization methods. 16

Since no oxycarbides had been reported for the lanthanide elements, and since their carbon systems were relatively well-known, with  $LnC_2$  being the most stable phase over the general temperature range of  $1000^{\circ}$  to  $2000^{\circ}$ , <sup>17</sup> earlier workers in this laboratory initiated equilibrium studies according to reaction (1) (in which M = Nd, x = 1.5, and y = 2). It was thought that few competitive processes would occur to complicate the study. The reaction was based on the familiar preparation of the dicarbide under vacuum first used by Moissan in 1896. <sup>4</sup>

This reaction was carried out in a closed, evacuated vessel, and did indeed appear to be an equilibrium process since the pressure of the system increased from zero to some constant value for a given crucible temperature. Investigation of the crucible contents by X-ray powder diffraction, however, showed the existence of the  $Nd_2O_3(s)$ , but no lines of the well-characterized  $NdC_2$ . Instead, an x-ray powder diffraction pattern that could not be indexed on the basis of any known neodymium-oxide or neodymium-carbide phase was observed.

This new phase, which was found to exhibit the stoichiometry NdOC, and its isostructural lanthanum analogue, LaOC are the basis for the experimental work reported in Chapter II of this thesis.

#### B. THEORETICAL CONSIDERATIONS

# 1. Thermodynamics 19, 20

The behavior of all heterogeneous physical systems at equilibrium is described by the phase rule of Gibbs,

$$f = c - p + 2,$$
 (2)

which summarizes the relationship between the number of phases present (p), the minimum number of components necessary to describe the system (c), and the degrees of freedom (f). The degrees of freedom specify the number of intensive, independent variables which describe the system.<sup>21</sup>

The system described in this part of the thesis, which will be shown to be

$$\text{Ln}_2 \circ_3(s) + 3C(s) = \text{Ln}_2 \circ_2 \circ_2(s) + Co(g),$$
 (3)

contains four phases (sesquioxide, graphite, oxycarbide, and carbon monoxide) and three components (lanthanide metal, carbon, and oxygen). Thus, there is but one degree of freedom, or one independent variable in the set of intensive variables describing the system. The activities of the solids are invariant, as will be shown, so only the variables of temperature and pressure are needed to describe the system. Since only one of these latter two variables is

independent, a unique pressure of carbon monoxide must be in equilibrium with the three solid phases at any given temperature.

By measuring the equilibrium carbon monoxide pressure as a function of temperature, the free energy change accompanying reaction (3) may be determined; with additional thermodynamic data, this measured free energy change can be converted to the standard free energy change for the given reaction. The standard enthalpy and free energy of formation for the oxycarbide at 298° can also be determined, by use of the measured free energy change and additional reported thermodynamic data.

## (a) Relationships from the Second Law of Thermodynamics

The standard free energy change for the reaction

$$\ell L + mM = qQ + rR \tag{4}$$

may be represented by

$$-\Lambda G_{T}^{\circ} = RT \ln K_{eq} = RT \ln \frac{a_{Q}^{q} a_{R}^{r}}{a_{L}^{\ell} a_{M}^{m}}$$
 (5)

where  $a_Q^q$  represents the activity of the equilibrium component Q in equation (4) raised to the power q, etc. In equation (3), all phases except carbon monoxide are solids having extremely low vapor pressures; therefore they can be considered to exist in their standard states, and to possess unit activities

(standard states for solids are usually defined as the pure solid in the most stable form at the specified temperature and a pressure of one atmosphere). If the gas pressures never exceed 0.5 atm. over the temperature range of interest, the pressure of the gas may be assumed identical with its fugacity and equation (5) may be re-written

$$-\Lambda G_{\rm T}^{\circ} = RT \ln P_{\rm CO(g)}. \tag{6}$$

Combination of this with the equation

$$\Lambda G_{T}^{\circ} = \Lambda H_{T}^{\circ} - T \Lambda S_{T}^{\circ}$$
 (7)

yields the equation

$$\ln P_{CO(g)} = -\frac{1}{RT} \wedge H_{T}^{\circ} + \frac{\Lambda S_{T}^{\circ}}{R}.$$
 (8)

It is apparent that a graph of the logarithm of the carbon monoxide equilibrium pressure versus the reciprocal of the corresponding absolute temperature will produce a straight line from whose slope and intercept  $\Delta H_{T}^{\circ}$  and  $\Delta S_{T}^{\circ}$  respectively may be deduced by assuming  $\Delta H_{T}^{\circ}$  to be constant over the temperature range of interest. The implications of this assumption will be investigated in the following section.

## (b) Heat Capacity Effects

The thermodynamic functions,  $\Delta H$  and  $\Delta S$  are always measured relative to some reference state which in this work will be the described system at a reference temperature  $\theta = 298.16\,^{\circ}F$ . In the general case, the heat capacity change  $\Delta C_{\rm p}$  at constant pressure (for one mole of product formed) is a function of temperature, and the relationships between the standard enthalpy and entropy at some temperature T and the reference temperature  $\theta$  are

$$\Delta H_{\rm T}^{\circ} = \Delta H_{\theta}^{\circ} + \int_{\theta} \Delta C_{\rm P} \, dT \qquad (9)$$

and

$$\Delta S_{T}^{\circ} = \Delta S_{\theta}^{\circ} + \int_{\theta} \Delta C_{P} \frac{1}{T} dT. \qquad (10)$$

Equations (9) and (10) are usually simplied by one of three assumptions. First, if  $\Lambda C_P = 0$ , the

$$\Delta H_{m}^{\circ} = \Delta H_{Q}^{\circ} \tag{11}$$

and

$$\Delta S_{T}^{\circ} = \Delta S_{\theta}^{\circ}, \qquad (12)$$

thus the plot of  $\ln P_{\text{CO}} = \frac{\text{vs.}}{T} = \frac{1}{T} = 1$  does in fact define a straight line of slope -  $\frac{\Delta H_{\text{T}}^{\bullet}}{R}$ . This assumption is probably valid only

over small temperature ranges. For larger temperature ranges, the plot of  $\ln P \ \underline{vs} \cdot \frac{1}{T}$  often shows curvature, and the assumption of  $\Lambda C_P = 0$  is inaccurate. Consequently, the second assumption is that the heat capacity change is not zero but is a constant function of temperature. By using this assumption, equations (9) and (10) are readily integrated, giving

$$\Delta H_{T}^{\circ} = \Delta H_{\theta}^{\circ} + \Delta C_{p}(T-\theta)$$
 (13)

and

$$\Delta S_{T}^{\circ} = \Delta S_{\theta}^{\circ} + \Delta C_{P} \ln(T/\theta).$$
 (14)

Equations (13) and (14) may be applied in the following manner: If the  $\ln P \ \underline{vs} \cdot \frac{1}{T}$  graph is relatively straight, but the mean temperature T is very much different from the reference temperature  $\theta$ , the measured slope and intercept, representing data taken at T must be corrected to the reference temperature by use of equations (13) and (14). If, however, the  $\ln P \ \underline{vs} \cdot \frac{1}{T}$  slope is not linear, the change in  $\Delta H^{\circ}$  and  $\Delta S^{\circ}$  resulting from heat capacity variation must also be included in the slope and intercept calculation. This is readily accomplished by the so-called " $\Sigma$ -Plot Method."

In this method, equations (13) and (14) are substituted into equation (8), which after collecting terms yields

$$-\text{Rln P} + \Lambda C_{\text{P}} \left[ \frac{\theta}{T} + \text{ln T} \right] = \frac{\Lambda H_{\theta}^{\circ}}{T} - \Lambda S_{\theta}^{\circ} + \Lambda C_{\text{P}}(1 + \text{ln}\theta). \quad (15)$$

Defining

$$\sum = R \ln P - \Delta C_P \left[ \frac{\theta}{T} + \ln T \right]$$

and

$$I = \Lambda S_{\theta}^{\circ} = \Lambda C_{P} [1 + \ln \theta]$$

and substituting these into equation (15) gives

$$\sum_{i} = \frac{-\Lambda H_{\theta}^{\circ}}{T} + I. \tag{16}$$

If this assumption is correct, a plot of  $\Sigma$  <u>vs</u>.  $\frac{1}{T}$  will produce a straight line of slope  $\Lambda H_{\theta}^{\circ}$  and intercept I, from whose definition  $\Lambda S_{\theta}^{\circ}$  may be deduced.

The third method involves writing  $^{\Lambda}C_{p}$  as an analytic function of temperature, followed by integration of equations (9) and (10). The results of these integrations are substituted into equation (8), followed by a treatment analogous to (but more difficult than) that used in the  $^{"}\Sigma$ -plot method." This treatment, though the most rigorous, is usually impossible in high temperature chemistry because of the lack of analytic functions for heat capacity relationships.

## (c) Relationships from the Third Law of Thermodynamics

Thermodynamic calculations may be made at various temperatures with the aid of the so-called "free energy functions," henceforth abbreviated fef, (where  $\theta$  is normally 298.16°K)

$$fef = \frac{\left(G_{T}^{\circ} - H_{\theta}^{\circ}\right)}{T} = -S_{T}^{\circ} + \frac{\left(H_{T}^{\circ} - H_{\theta}^{\circ}\right)}{T}$$
(17)

and experimentally-determined enthalpies and free energies of formation. This method is particularly useful in calculations involving high temperature thermodynamics for several reasons:

- 1. It provides a compact method of storing large amounts of thermal data covering wide temperature ranges, since the fef varies smoothly with temperature. Hence only relatively few fef points need be tabulated vs. temperature for construction of a graph from which fef values may be deduced.
- 2. If the required fef's are available for the computation in question, the enthalpy calculated by their use is independent of the enthalpy calculated by the second law method outlined previously, since the fef's are dependent on third-law calculations. This dependency will be demonstrated.

- 3. If all required fef's are available, the possibility of complicating reactions such as sample crucible interaction can be investigated.
- 4. If an fef is unavailable, but can be approximated by analogy, third law enthalpies can still be calculated. These enthalpies, though possibly inaccurate in absolute value, still establish an independent check of second-law equilibrium data.

The dependence of this method on third-law information can be seen by the fact that the right side of equation (17) can be evaluated by the third-law method of integrating heat capacity data from T=0 to T=T, the temperature in question. The first term may be evaluated as follows:

$$S_{T} = \sum_{Q}^{T_{1}} \frac{C_{P}}{T} \Delta T + \int_{T_{1}}^{T_{Q}} \frac{C_{P}}{T} dT + \frac{\Delta H_{tr}}{T_{Q}} + ... + \int_{T_{1}}^{T} \frac{C_{P}}{T} dT. \quad (18)$$

The summation term is an approximation to the integral

$$\int_{0}^{T_{1}} \frac{C_{P}}{T} dT. \quad T_{1} \text{ is usually selected to be a very low temperature}$$

(some tens of degrees) and the first term evaluated either graphically or by a Simpson's rule summation. The second

term of the right side of equation (17) can be evaluated by a similar computation.

$$\left(\frac{H_{T} - H_{\theta}}{T}\right) = \frac{1}{T} \left[\int_{\theta}^{T_{1}} C_{P} dT + \Lambda H_{tr} + \int_{T_{1}}^{T_{2}} C_{P} dT + \ldots + \int_{T_{1}}^{T} C_{P} dT\right]. \quad (19)$$

In the thid-law method, problems arise when a needed fef is unknown and cannot be estimated with any degree of certainty, because of a lack of thermodynamic information about related compounds. In such cases, a model of the particular phase is postulated and an fef based on that model is calculated. If the fef appears reasonable, the enthalpy value computed from this fef can be used as an independent corroboration of the value computed by the second-law method. The amount of confidence placed in the numerical values resulting from such a calculation will be related to the information supporting the model used.

## 2. <u>Instrumental Theory</u>

## (a) Optical Pyrometry

Planck's general law of radiation for a black body is

$$J_{\lambda,T} = \frac{c_1}{\lambda^5 \exp(c_2/\lambda T) - 1}$$
 (20)

where

$$C_1 = 2\pi \ln c^2$$

$$C_2 = hc/k,$$

c is the speed of light, and  $\lambda$  is the light wavelength. This equation describes the intensity of a black body radiator as a function of wavelength and temperature. If the wavelength is held constant in equation (20), the intensity  $J_{\lambda,T}$  will be a unique function of temperature. This law is the basis for the monochromatic optical pyrometers used to obtain all the experimental temperatures reported in this work. A red filter transmits a band of wavelengths around 6500 A, and the intensity of this band is compared with that of a standard filament viewed through the same filter. The intensity of the standard filament which is superimposed on the image of the source is adjusted by a slide wire until the two are of the same intensity. The voltage drop across the standard filament is then compared with a standard cell and the temperature read from the calibrated slide-wire. The measurements made by such a instrument have been found reproducible to ±2° up to 1750°. When the instrument is calibrated against NBS\* standards, measurements are presumed accurate within the

<sup>\*</sup> National Bureau of Standards

standard deviation of the measurement and the error limits established by the NBS for its standards at the measured temperatures. The radiation measured, is assumed to emanate from a perfect black body radiator.\*

### (b) Absorption Corrections in Pyrometry

correction of radiation for absorption by the external optical system is most easily accomplished empirically, since the constants needed are difficult to calculate. A combination of Beer's law for absorbance and Wien's law of radiation, which is an empirical law more easily handled than Planck's, is used for the correction. Wien's law predicts intensities which are within 1% of the true values in the spectral region utilized in the monochromatic pyrometer.

The following relationship between true temperature T and observed temperature  $T_a$  viewed through an absorber is derived as indicated above:

<sup>\*</sup> This assumption can be supported by using the approximation that the number of internal reflections occurring before escape of a given quantum of radiation is represented by the ratio of the area of origin to that of the cavity interior. (In a typical crucible used throughout the work reported in this thesis, this ratio had a value of greater than 700.)

$$\frac{1}{T} - \frac{1}{T_a} = \frac{\lambda \ln \tau}{C_2} . \tag{21}$$

The transmittancy of the absorber is represented by  $\tau$ . Since the transmittancy is invariant for a monochromatic pyrometer, the entire right side of this equation is constant, and equation (21) can be written

$$\frac{1}{T} - \frac{1}{T_a} = C. \tag{22}$$

This equation allows a very simple experimental determination of C for a set of points defined by T and  $\mathbf{T}_{\mathbf{a}}$ .

#### (c) Two-Color Pyrometry

Since the intensity of a particular wavelength of black-body radiation defines the temperature of that body, the ratio of intensities of two different wavelengths can also be shown to define a black body temperature. The major advantages of two-color pyrometry are:

- 1. The temperature measured is independent of the absorber so long as the absorber does not selectively transmit one of the two wavelengths used.
- 2. In the absence of a black body radiator, the correction term ε, denoted the "emittance" of the body, relates the flux characteristic of the

true temperature,  $J_{\lambda,T}$ , to the observed flux of a non-black body radiator,  $J'_{\lambda,T}$ . The equation is

$$J_{\lambda,T}' = \varepsilon J_{\lambda,T}. \tag{23}$$

In two-color pyrometry, the ratio of two fluxes is measured as is indicated in equation (24),

$$\frac{J_{\lambda_{1,T}}}{J_{\lambda_{2,T}}} = \frac{\varepsilon_{1}^{J_{\lambda_{1,T}}}}{\varepsilon_{2}^{J_{\lambda_{2,T}}}}.$$
 (24)

If it can be shown that  $\epsilon_1$  and  $\epsilon_2$  are equal,

the emissivity corrections cancel, allowing true black body temperatures to be measured from surfaces.

## C. EXPERIMENTAL METHODS, Ln<sub>2</sub>O<sub>2</sub>C<sub>2</sub>

### 1. Synthesis

Preparatory techniques used in synthesizing the Ln<sub>2</sub>O<sub>2</sub>C<sub>2</sub> phase were developed over a period of several years. Improvements in product purity, ease and speed of preparation, and reproducibility were due almost entirely to the availability of new instruments during the time involved. For this reason, the various preparatory methods will be described individually in chronological order along with descriptions of the instruments employed in that particular synthesis. Several general instrumental techniques used in most of the work reported will be described separately.

## (a) Starting Materials and Their Handling

Materials used in the preparation of the oxycarbide phases were the lanthanide metals in ingot form, lanthanum (99%), neodymium (99%); the corresponding powdered sesquioxides of lanthanum (99.9%) and neodymium (99.9%), and grade no. 38 graphite powder. Sources of these materials are listed in Appendix I.

The sesquioxides tend to absorb carbon dioxide from the atmosphere to form the metal carbonates. Since

appreciable amounts of such carbonate impurity would lead to incorrect amounts of the metal and oxygen in the preparatory mixtures, the oxides were calcined at 900° in platinum crucibles for a minimum of eight hours in a muffle furnace. The crucibles were then cooled and stored in desiccators. The metal ingots were stored in a vacuum desiccator and were exposed to air for minimal time when samples were removed from the stock material. Metal samples of 0.5-1.0g were removed from the ingots either by cutting pieces of the approximate size required with a clean and sharp cold chisel, or by filing with a previously cleaned, coarse mill file. Samples prepared by the filing method were subjected to magnetic cleaning to remove possible contaminants chipped from the file. To minimize contamination by surface oxidation, metal samples were used either immediately or stored in a vacuum desiccator for no longer than one day. The graphite powder was used without further purification.

## (b) General Techniques

Described here are techniques and instruments which will be referred to throughout the remainder of this thesis, and will be noted only briefly subsequent to these descriptions. Other more specific techniques will be described in the context of their use.

- Moisture. Many manipulations had to be carried out in the absence of atmospheric moisture and/or oxygen, due to the great reactivity of some of the materials studied. For such manipulations, a helium-filled glove-box was employed. The helium in this glove box was dried over phosphorous pentoxide and recirculated through a system which employed molecular sieve drying columns. Samples which would have hydrolyzed or oxidized very rapidly in the air were brought into the dry box quickly after removal from the apparatus in which they were prepared. Exposure to air never exceeded about fifteen seconds for such materials. In all following descriptions, the term "glove box" refers to this apparatus.
- (ii) Temperature Measurements. Except for a few relatively low temperature (600 1000°) measurements for which thermocouples were employed, all temperatures reported in this thesis were measured by a model 8622-C Leeds and Northrup disappearing-filament-type pyrometer (serial no. 1572579). This pyrometer had been calibrated at the NBS, and its calibration was checked by comparing it to a similarly calibrated instrument reserved for comparison purposes. A tungsten strip lamp powered by

a voltage-stabilized source which had a six-step ouput was used for comparative measurements. The temperature of the strip lamp was measured by the two pyrometers at each of the six temperatures produced by the stepped-output transformer. Care was taken to measure the temperature of an identical section of the tungsten strip each time. From the correction data supplied by the NBS a calibration curve was constructed to enable comparison of the two pyrometers.

A similar technique was used for correcting the observed temperature when readings were taken through a prism and an optical window. The temperature of the tungsten strip was determined at each of six temperatures, by viewing the strip, first directly, then through the window-prism combination.

These data were used with equation (22) which relates absorbancy to temperature change, and the constant C for the prism-window combination was determined. With this constant a curve which covered the temperature range of 900 - 2200° was prepared to relate correction values to the observed temperature. This curve was combined with the NBS calibration curve for this pyrometer. This overall correction curve was then used for all measurements requiring that particular optical arrangement.

(iii) Metallography (Micrography). Micrography is a general technique used to prepare and examine crosssections of fused materials. Samples were mounted in Met-A-Test cold mount material (Precision Scientific Co., 3733 W. Cortland St., Chicago, Ill.). When the mounts had hardened, the samples were ground on a Precision Scientific Co. electric polisher, by using successively numbers 180, 320 and 600 abrasive papers; then polished on a fiber platten charged with number 600 abrasive powder. If magnifications of 800x or greater were to be used, a final polish was effected on a Buehler Vibromet polisher (Buehler Ltd., 2120 Greenwood St., Evanston, Ill.) by using 1.0 micron alumina abrasive.

During grinding and polishing operations, the sample was bathed continuously with a thin, anhydrous mixture of paraffin oil in kerosene. This mixture was flowed in a thin stream onto the abrasive surface in front of the sample. This lubricant provided a solvent for the abrasive operation and also prevented hydrolysis of the sample surface by atmospheric moisture. This lubricant was continuously filtered, dried and re-circulated by a peristaltic-type pump.

The polished face of the sample was washed thoroughly in a stream of the freshly-filtered kerosene

mixture, the excess was wiped off and a microscope slide cover glass was placed over the polished sample surface to prevent hydrolysis. If a permanent sample was desired, the cover glass was affixed with a drop or two of Canada balsam. Interpretation of micrographs will be discussed later in this chapter.

(iv) X-Ray Powder Diffraction. These techniques, henceforth referred to as "x-ray diffraction" in this thesis, were used in the preparatory development, but will be described in the analytical section.

#### (c) Containers

Except where otherwise noted, the containers used both for preparatory methods and later for equilibrium studies were cylindrically-shaped graphite crucibles of 2 cm diameter and 3 cm height, with walls of at least 5 mm thickness. The crucibles were covered with close-fitting graphite lids of at least 5 mm thickness, with a 0.8 mm hole drilled axially. This lid permitted gases to escape and provided a line of sight into the crucible cavity for temperature measurements. These crucibles were outgassed in the system described in Appendix II to a temperature of  $2000-2050^{\circ}$  and an accompanying pressure of less than  $5 \times 10^{-6}$  torr for a period of not less than

three hours. Graphite served as a good crucible material for the following reasons:

- 1. Graphite contamination did not affect subsequent analysis of the product.
- 2. In equilibration studies, graphite was shown to be one of the solid components of the equilibrium mixture, and the crucible therefore could not contribute any interfering contaminants to the process being studied.

Different crucible materials were used infrequently, and they will be described in the context of their use.

#### (d) Synthesis I

This procedure was developed during the discovery of the phase and is therefore somewhat crude. The pelletized lanthanide sesquioxide and graphite mixture was placed in an outgassed graphite crucible which was positioned on a boron nitride support. A double-walled, water-cooled Vycor tube fitted with an optical window at its top surrounded the crucible and permitted attainment of a pressure of approximately 10<sup>-5</sup> torr. An oil diffusion pump and a mechanical backing pump completed the vacuum unit. Since it was found that the reaction did not proceed at a measurable rate below 1300°, as evidenced by a stable pressure in the system

when it was evacuated, closed and maintained at that temperature, the reactants were outgassed by heating the crucible and contents at 900 - 1000° under vacuum for 30 minutes. system was then sealed and the crucible quickly heated to the desired operating temperature at which it was maintained for 3.5-5 hours. When the product had cooled, it was transferred to the glove-box and a small representative portion of the pellet was removed for x-ray diffraction analysis. sesquioxide was present, the remaining sample was placed back into the heating system, and the previous procedure was repeated; except that after the operating temperature had been reached, some of the gases produced by the reaction were pumped off. The pressure change due to gas removal was monitored by a stainless steel absolute pressure manometer (Wallace & Tiernan model FA-145). Usually two such pump-offs were required for a 3g sample before the intensity of x-ray diffraction lines attributable to the sesquioxide faded to a minimum value.

# (e) Synthesis II

This method is a further development of synthesis I, made possible by the availability of a new equilibrium system which permitted the achievement and maintenance of internal gas pressures from  $5 \times 10^{-7}$  to 700 torr. (This is the same system that was later used for equilibrium experiments and its operation will be described fully in

that section). The procedural modifications made possible by this new apparatus were suggested by the concept that an equilibrium system was being studied, and maintenance of the gas pressure below the equilibrium value at the given temperature should induce complete reaction and yield a product free of reactant material. In addition, the procedure would be well-defined and reproducible (which synthesis I was not). Analytical investigations on samples prepared by synthesis I had indicated probable composition of Lnoc. Therefore samples of sesquioxide and graphite were mixed according to the stoichiometry predicted by the equation

$$\text{Ln}_2 O_3(s) + 3C(s) \rightarrow \text{Ln}_2 O_2 C_2(s) + CO(g).$$
 (26)

Procedures employed were similar to those of synthesis I except that after the initial outgas of the crucible and contents, the system was sealed and the temperature was elevated to about 1600°. The sample was heated until the pressure had remained constant for at least one hour. This pressure was assumed to define an equilibrium state at that temperature. Carbon monoxide was then slowly pumped from the system until the pressure of carbon monoxide had fallen about 10 torr, after which the system was again sealed and the pressure rise monitored.

This procedure was repeated until the pressure no longer increased to the original value after removal of carbon monoxide, and was indicative of a lack of equilibrium conditions. The crucible was allowed to cool, the system was first evacuated and then brought to atmospheric pressure by the addition of helium, and the crucible and its contents transferred to the glove box.

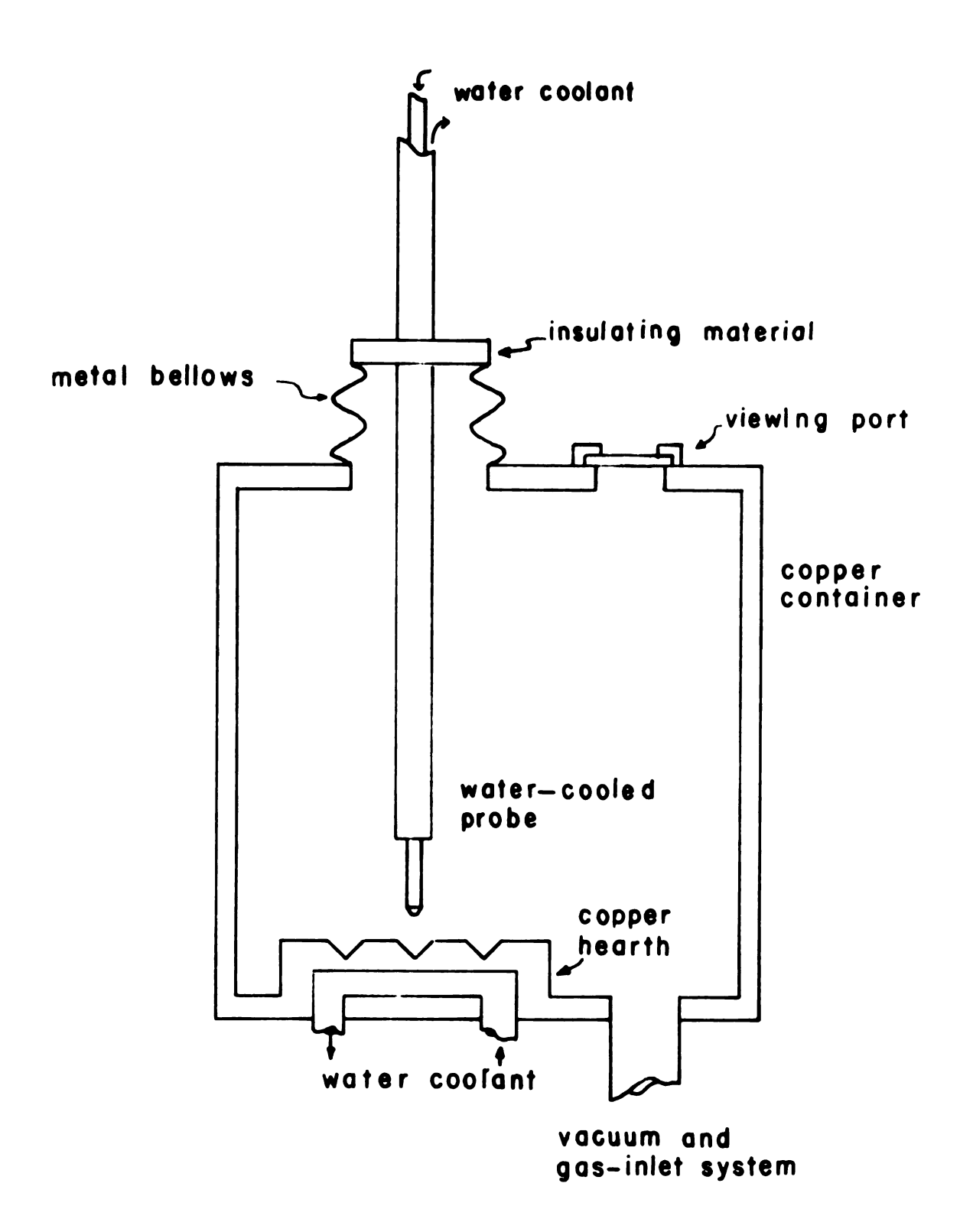
Samples prepared by this synthetic method exhibited only extremely faint sesquioxide lines. assumption that incomplete reaction was a result of inhibition of the reaction by slow diffusion across the graphite sesquioxide interface, the preparation was attempted at increased temperatures but with little improvement. At about 1850°, a vigorous reaction which always occurred between the sample and the crucible wall, formed a fused gold-colored material and eroded (sometimes completely through) the crucible walls. This erosion occurred simultaneously with the fusion of the oxycarbide sample, since portions of the product not in direct contact with the wall were also fused. X-ray investigation of the fused oxycarbide not in contact with the wall showed the complete absence of sesquioxide x-ray diffraction lines and suggested the use of some technique involving fusion.

Availability of an arc melter (Fig. 1) made such a synthesis feasible (synthesis III). Study of the fused, gold-colored material formed by reaction of the sample and the wall will be discussed in the context of equilibrium studies (cf. pp. 57).

#### (f) Synthesis III

The arc melt technique is in principle quite simple. It consists of fusing a mixture of the desired composition with a direct current arc, struck between a negatively-charged, water-cooled copper hearth on which the sample mixture sits and a water-cooled graphite or tungsten electrode. As soon as the sample mixture began to fuse, its conductivity increased sufficiently so that the arc could be maintained between the electrode and the sample, thereby producing the beneficial result of heating the sample to a very high temperature without heating the copper hearth excessively.

The electrode is attached to the arc melter chamber by a flexible metal bellows, and if the pressure differential between the chamber interior and the atmosphere is more than about .1 atmosphere, the electrode is either jammed against the hearth or held a distance away from it (more than 5 cm). Either way makes maintenance of the proper arc-length of 1 cm very difficult. For this reason, internal gas pressures very near atmospheric had to be used. In the arc melt preparations of  $\operatorname{Ln}_2O_2C_2$ , the



# ARC-MELTER ASSEMBLY

Figure 1.

chamber was filled to a pressure of one atmosphere with carbon monoxide, thus maintaining both ease of electrode manipulation and the caron monoxide pressure requirements of the fused oxycarbide. The toxicity of this gas required that the chamber be flushed (with either nitrogen or helium) before opening, and that the vacuum pump be exhausted into a hood.

The initial sample was prepared according to the stoichiometry of equation (3), the sesquioxide and graphite being pelletized as before and arc-melted. The x-ray diffraction pattern of the preparations exhibited sesquioxide lines which could be minimized (but not eliminated completely) by diluting the carbon monoxide in the melter chamber with successively larger fractions of helium. While the sesquioxide x-ray diffraction lines were still visible at low partial pressures of carbon monoxide, the Ln<sub>2</sub>O<sub>2</sub>C<sub>2</sub> x-ray diffraction lines disappeared completely and a set of lines indicating cubic symmetry appeared together with the sesquioxide pattern. The persistence of the sesquioxide phase was not surprising at the higher partial pressures of carbon monoxide, since this behavior appeared to be analogous to the equilibrium formation observed in syntheses I and II, though the atmosphere of an arc can hardly be considered an equilibrium system. The cubic phase which appeared is considered in detail in chapter III

of this thesis. The need for a preparatory procedure in which no carbon monoxide is liberated, thus minimizing equilibration, led to preparations based on the stoichiometries indicated by the equation

$$Ln(s) + Ln_2O_3(s) + 3C(s) \rightarrow 3/2 Ln_2O_2C_2(s)$$
. (26)

Samples were prepared in either of two ways:

- 1. Metal filings were mixed with the sesquioxide and graphite, then the mixture was pelletized.
- 2. The metal was used in single (0.5 1.0 g) pieces and melted together with pelletized sesquioxide and graphite mixtures.

Samples prepared via alternative (2) were indistinguishable both micrographically and by x-ray diffraction from those prepared by number (1). Since metal filings were assumed more susceptible to oxidation prior to use, and were, in addition, more difficult to make from stock metal ingot, the second alternative was preferred. On the basis of phase purity studies (discussed in the following section), this method was judged to produce the best samples of the  $\operatorname{Ln}_2O_2C_2$  phase and was employed for preparation of all samples used for further studies.

# (g) Synthesis IV

Another preparatory scheme involved samples mixed according to stoichiometries indicated by

$$Ln_2O_3(s) + LnC_2(s) + C(s) \rightarrow 3/2 Ln_2O_2C_2(s)$$
 (27)

and arc-melted under a one atmosphere pressure of CO. starting mixture was difficult to handle, since the LnCo and  $\operatorname{Ln}_2\operatorname{O}_3$  had to be weighed, mixed and placed in the pellet press in a glove box to prevent hydrolysis of the The LnC, was prepared by heating the lanthanon and dicarbide. carbon in 1:2 mole ratios in a tantalum bomb at 1700° for four hours. The bomb was opened and the product stored in the glove box. The pellet press was loaded in the glove box, enclosed in several layers of thin plastic sheet, then was removed from the glove box and the sample subjected to a pressure of about 2500 psi. The pellet press was then returned to the glove-box where the pressed pellet was removed and sealed in a vial. The vial was fractured immediately prior to evacuation of the arc-melter, and the pellet of Ln<sub>2</sub>O<sub>3</sub> and LnC<sub>2</sub> were exposed to air for not more than ten or fifteen seconds.

# (h) Synthesis V

The final preparatory technique was inspired by questions concerning the possibility of metal carboyl formation. The Ln metal was arc melted in a carbon monoxide atmosphere to investigate this possibility. The fused sample was fractured and re-melted several times to promote homogeneity.

#### 2. Phase Purity

Several experimental techniques are used to obtain information concerning identity of phases present in a particular material. Very few of these techniques if used alone permit the complete characterization of the phases. In the present work, it was necessary to determine when a preparatory procedure produced a phase that was monophasic within the limits required for analysis. These limits require than an impurity, such as graphite, which can be determined independently, is acceptable only when present in amounts low enough that indeterminancy in free-carbon determinations will not affect the results of the other analyses. On the other hand, the sesquioxide or the dicarbide cannot be differentiated analytically from the phase to be determined, thus they may be present only in amounts so small that the error they introduce is less than the standard deviation of the measurements. Thus most phase-purity investigations were physical, since chemical separation is excluded as the preceding discussion indicates.

X-ray diffraction (discussed in detail in the analytical section) is a powerful qualitative tool for phase determinations, but quantitatively the relative pattern intensity of two phases cannot be related directly

to the relative amounts of the phases present, since diffraction line intensity is also related to other factors, such as structure type, self-absorption, and thermal motion. As long as a minor component is present in an amount greater than 15%, the diffraction pattern of that phase usually can be observed. Thus x-ray diffraction is very useful only for initial phase analysis within the stated limits.

Another useful tool, within limits, is micrography. As long as the phases are immiscible and are or can be made differentiable by some visual method, the phase purity can be investigated. If a solid solution exists, its presence can be shown by variation of a lattice parameter which is determined by x-ray diffraction.

In the preparatory investigations, x-ray diffraction was utilized to enable gross purification of the oxycarbide from the lanthanide dicarbide and lanthanide sesquioxide phases. Further refinement of preparatory methods was accomplished micrographically. The oxycarbide showed no apparent shift in lattice parameter when the LnC<sub>2</sub> or Ln<sub>2</sub>O<sub>3</sub> were shown to be present by x-ray diffraction: thus it was judged that micrography could be used to show the presence or absence of these phases if they could be differentiated visually from the Ln<sub>2</sub>O<sub>2</sub>C<sub>2</sub> phase. The LnC<sub>2</sub>

phase was identifiable by its gold color, in contrast to the metallic grey of the oxycarbide. The sesquioxide was identified by allowing the polished surface of the sample to tarnish by exposure to air for a few seconds. The color of the sesquioxide remained unchanged in contrast to the colors of the dicarbide and oxycarbide which became dull quickly.

estimates of their apparent ratios in the samples as determined by the area each covered in the micrographic section allowed phase purity estimates to be made in the various synthetic schemes. Such investigations were also used to determine the effect various electrode materials and 'time at arc temperature' had on sample purity.

#### 3. Analytical Procedures

Ternary phases such as Ln<sub>2</sub>O<sub>2</sub>C<sub>2</sub> consisting of a relatively heavy metal and two light non-metals pose analytical problems of some magnitude, particularly when one of the non-metals is oxygen. The problems are due to:

- 1) cumulative errors inherent in any difference determination,
- 2) difficulty in analyzing directly for oxygen
- 3) small errors in the relative percentages of the nonmetals which produce large errors in the stoichiometry deductions.

Analysis of this particular phase was complicated further by the rapidity with which it hydrolyzed. This property required that all analytical samples be prepared and weighed in the glove-box.

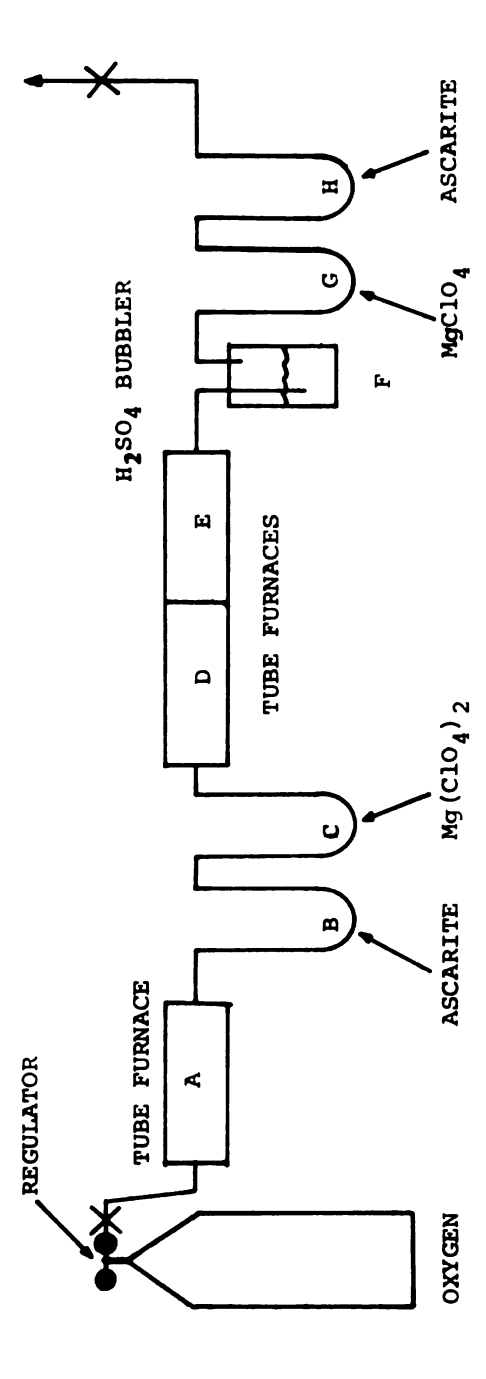
Fused ingots of the Ln<sub>2</sub>O<sub>2</sub>C<sub>2</sub> were fractured initially with a hardened steel mortar which had a retainer sleeve to prevent material loss. The sample was then pulverized in a large Diamonite mortar. As many as six 1 g samples were prepared at one time, and then were taken into the glove box, where they were pulverized and mixed together intimately to produce one homogeneous sample. Such a preparation furnished four samples for metal analysis and at least three samples for total carbon or oxygen analysis.

(i) Metal Analysis. In the glove box, four weighed samples of 0.5 to 0.8 g were placed in 400 ml beakers which were then covered with watch glasses to prevent accidental contamination, and removed from the glove box. Since these portions were to be hydrolyzed, no attempt was made to exclude air. Hydrolysis was effected by the slow addition of 125 ml of 1N HCl; the samples were digested on a hot plate for not less than four hours, and allowed to cool. The contents of the beakers were filtered through tared alundum filter

crucibles to remove free carbon; the crucibles were dried subsequnetly at 100° for at least 6 hours, cooled and the increase in mass considered as free carbon. crucibles were then fired at around 900° for a minimum of 4 hours to oxidize the filtered carbon, cooled, and weighed. The weight loss, interpreted as free carbon, provided a check on the previous determination. Dilute ammonium hydroxide was added to the filtered solutions until the methyl orange end point was reached (usually small amounts of hydroxide precipitate could be observed at this point). Twenty-five ml of concentrated oxalic acid was added slowly with stirring; the samples were covered and digested on a hot plate for at least six hours. Completeness of precipitation was determined by adding an additional lml of oxalic acid to the cooled supernatant solutions. If no precipitate formed (normally the case), the solutions were filtered through tared alundum filter crucibles, which were first dried, then heated slowly by a Meker burner to prevent too rapid evolution of carbon dioxide with attendant material loss. The crucibles were finally ignited to 900° for at least twelve hours, to convert the oxalate to the sesquioxide. The crucibles were cooled in a desiccator for two hours, then weighed.

(11)Total Carbon Analysis. Total carbon content of the samples was determined by a combustion technique, by use of the apparatus illustrated in Fig. 2. Oxygen (USP) was admitted to the system at pressures of less than one psi and at flow rates of 6-8 ml/minute. Any carboncontaining impurities in the oxygen were oxidized over a CuO-CeO, catalyst maintained at about 750° in furnace (A), and water or carbon dioxide formed by this pre-oxidation were absorbed in U-tubes (B) and (C) containing respectively  ${\rm Mg(ClO_4)_2}$  and Ascarite. A sample to be analyzed was placed in furnace (D) and heated in the stream of pure, dry oxygen. Any carbon in the sample was oxidized to carbon monoxide, carbon dioxide or a mixture of the two gases, and then swept over a CuO-CeO, catalyst maintained at 750° in furnace (E), where any carbon monoxide gas present was oxidized to the dioxide. The oxygen-carbon dioxide gas mixture was dried in the  $H_2SO_{j_1}$  column (F) and the  $Mg(ClO_{j_1})_2$ filled U-tube (G), and then swept through the tared Ascarite filled U-tube (H), in which the carbon dioxide was absorbed. This U-tube was then weighed, and the total carbon content in the sample was determined.

In a typical experiment a 0.6 - 0.8 g portion of the original homogeneous sample was placed in the



CARBON ANALYSIS SYSTEM

FIGURE 2. Combustion Apparatus

approximate center of the Vycor tube in furnace (D). which was initially at room temperature (in contrast to furnaces (A) and (E), which were maintained at about 750°). The system was closed, and the oxygen flow was initiated and maintained at about 6 ml/min. The sample temperature was elevated over a 5-hour period to just over 1000°, then maintained at this level until the absorber weight as indicated by hourly weighings was constant (or the weight gain had decreased to the predetermined "blank rate"). The accuracy of this analytical procedure and the "blank rate" were determined using out-gassed graphite and calcium carbonate as known carbon sources. absorber connections were arranged so that the inlet and outlet tubes could be connected when the absorber was weighed, thus preventing the absorption of atmospheric moisture by the ascarite. This arrangement also allowed rapid closing of the system. The absorber was always attached and detached as quickly as possible, and was handled with plastic-coated cotton gloves to minimize weight gains due to fingerprints.

(iii) <u>Hydrolysis Experiments</u>. A sample of the oxycarbide was hydrolyzed by water vapor and the gases so produced were collected. These gases were analyzed using an F & M Scientific Corp. flame-ionization-type gas chromatograph (Model 615) which had been standardized with ethane and acetylene.

(iv) X-Ray Investigations: The oxycarbide phase was examined both by Debye-Scherrer cameras and recording diffractometers. In each case, sample preparation stressed exclusion of atmospheric moisture to prevent hydrolysis. Capillaries 0.3 mm in diameter were loaded in the glove box, placed in sealed vials and flame sealed immediately upon removal from the vials. Debye-Scherrer cameras of 114.59 mm diameter were used, with copper K $\alpha$  radiation ( $\lambda\alpha_{II} = 1.5418$  Å).

Samples were prepared in the glove box for diffractometry by pressing a powdered sample into a rectangular 2.5 x 0.5 cm cavity machined 2 mm deep into a brass sample holder. The sample was smoothed and covered with a strip of Scotch "magic mender" tape. The tape was shown to prevent noticeable hydrolysis for up to two hours. For longer diffractometer runs, a thin coating of paraffin oil was flowed over the tape. This procedure prevented noticeable hydrolysis for up to eight hours. A Siemens diffractometer was equipped with a scintillation detector whose output was monitored by a pulse height analyzer in an attempt to reduce the fluorescence background of the sample.

- (v) <u>Infrared Studies</u> An infrared spectrum was obtained on a Unicam SP 200 spectrometer using the KBr pellet technique. The KBr press was loaded in the glove box, removed and the sample pressed under vacuum. The disc was subjected immediately to infrared analysis. Since atmospheric moisture could not be excluded from the sample compartment of the spectrometer, slight hydrolysis occurred on the disc surface.
- (vi) Equilibrium Studies The system used for equilibrium studies is described fully in Appendix (II).

  Briefly, it consisted of a 100 mm diameter Pyrex tube which confined a water-cooled current concentrator suspended from a brass, water-cooled lid which contained an optical window that could be magnetically shuttered from exposure to the hot crucible. The crucible was supported in the center of the copper donut on 1.52 mm diameter tungsten legs about 2 cm long. The pressure measuring system consisted of the Wallace and Tiernan dial manometer described previously and an absolute pressure U-shaped mercury manometer whose column height difference was determined with a Gaertner Scientific Co. Model M-908 cathetometer. The mercury manometer was employed to check the dial manometer at low pressures. Compressed gas from a tank was

admitted to the system through a  $Mg(ClO_4)_2$  drying column and a flow-meter. This gas-handling system allowed very precise monitoring and control of gas pressures.

Temperature control was achieved for the  $\mathrm{La_2O_2C_2}$  study by use of a two-color pyrometer (Latronics Corp., Latrobe, Pa.). This pyrometer monitored the total emission of the crucible lid through the Pyrex tube at an oblique angle so that temperature measurements of the crucible cavity could be made without interrupting the control achieved by the pyrometer. The output of the two-color pyrometer was led into a Model 90 Leeds and Northrup automatic controller, in which the pyrometer signal was balanced against a Zener diode. Any excursions from the null point due to temperature variation generated a signal which altered the furnace output so as to reverse the variation. The two-color pyrometer had internal calibration checks on both sensing circuits. bration was checked regularly; every thirty minutes at the beginning of an equilibrium experiment and less frequently thereafter as the circuitry stabilized.

This temperature control unit was not available when equilibrium measurements were made on the  $\mathrm{Nd_2O_2C_2}$  system. The control unit accounts for the improvement in the scatter of the  $\mathrm{La_2O_2C_2}$  data, since previously it was

difficult to maintain the temperature at a constant value for several hours.

A finely pulverized  $Ln_2O_2C_2$  sample (1.4 - 2g) was inserted into a graphite crucible in the glove box, then the crucible was placed in the equilibrium system which was immediately evacuated. The crucible was subjected to a final outgas by heating in vacuum at just under 1000° for approximately two hours, after which the equilibrium system was valved from the pumping system. Sufficient carbon monoxide (Matheson, CP) was added to the equilibrium system to achieve a pressure of 70 - 100 torr, and the crucible was then heated to some pre-determined temperature above 1350°. When the carbon monoxide pressure in the system had stabilized, portions of carbon monoxide were removed or added, thereby reducing or increasing the carbon monoxide pressure by 3-10 torr increments, and the system was then allowed to re-stabilize. During this entire procedure, the temperature was maintained at a constant value. When a given pressure was re-established to within ±0.3 torr after both high and low pressure excursions at a constant temperature, that particular pressure and the corresponding temperature were assumed to define a reversible state. Small gas samples were removed

periodically from the equilibrium system by expanding a small amount of the gas into an evacuated 1 liter flask via a manifold on the gas inlet line. This gas sample, which was in equilibrium with the crucible contents, was analyzed mass spectrometrically. If the gas sample proved to be carbon monoxide, the reversible state demonstrated at the particular temperature and pressure was assumed to be an equilibrium state.

This procedure was repeated for a series of temperatures, taken in a generally random order. Seven to twelve pressure-temperature pairs defining equilibrium states were recorded for each sample, and at least three different samples were subjected to equilibration study for both  $\text{La}_2\text{O}_2\text{C}_2$  and  $\text{Nd}_2\text{O}_2\text{C}_2$ .

Small portions of the crucible contents were removed periodically after equilibrium conditions had been exhibited to determine the solid phases which exist in equilibrium with carbon monoxide gas. At gas pressures exceeding approximately 130 torr, pressure fluctuations were detected. By heating an empty crucible in similar helium pressures, these fluctuations were shown to exist independently of the chemical system being studied. The fluctuations were damped by partially closing the needle valve between the manometers and the equilibrium system.

# D. RESULTS OF Ln<sub>2</sub>O<sub>2</sub>C<sub>2</sub> INVESTIGATIONS

#### 1. Preparative Results

The original preparatory technique developed by G. L. Buchel and modified by the writer was unsatisfactory for the following three reasons.

- 1. Because of the heterogeneous solid solid reaction involved, the sample couldn't be prepared completely free of sesquioxide.
- 2. The technique involved trial and error methods which couldn't be standardized or repeated to prepare uniform samples.
- Micrographic analysis was impossible without a fused sample.

The arc melt technique proved to be a great improvement over previous methods. It produced samples which were free of sesquioxide x-ray diffraction lines, it was reproducible, and up to eight grams of sample showing good uniformity in x-ray and micrographic analysis could be prepared rapidly. Of the various preparations used, the one mixed according to stoichiometrics indicated by the equation

$$Ln(s) + Ln_2O_3(s) + 3C(s) \rightarrow 3/2 Ln_2O_2C_2(s)$$
 (28)

gave a product which showed greatest phase purity by both x-ray and micrographic analysis, and which also required less exacting preliminary care since the starting mixture could be handled with reasonable precautions in air. deposits of sesquioxide on the interior of the arc-melter chamber indicated that metal and/or metal monoxide gas were being lost preferentially by the sample during melting. Micrographic examination showed small amounts of a black phase (later shown to be graphite) distributed through the oxycarbide. The amount of graphite could be minimized by arc-melting the sample only long enough to produce homogeneous specimens. Samples arc-melted for about 35 seconds, which were turned over and remelted for another 35 seconds showed minimal amounts of graphite. Graphite, however, interfered with neither the analytical results, since bound and unbound carbon were determined independently, nor with equilibrium results, since graphite was one of the solid components in the equilibrium mixture.

The sample mixed according to the equation

$$\text{Ln}_2\text{O}_3(s) + \text{LnC}_2(s) + \text{C}(s) \rightarrow 3/2 \text{Ln}_2\text{O}_2\text{C}_2(s)$$
 (29)

was also arc-melted according to the above procedures. This method produced the oxycarbide but the product showed no improvement in purity over the method previously described

and the technique was discarded because of the already mentioned difficulties in preparing the sample mixture. That the  $\text{Ln}_2\text{O}_2\text{C}_2$  has narrow composition limits was shown by the position invariance of the various back-reflection lines in the x-ray diffraction patterns shown by samples containing excess metal, oxide or graphite.

Arc-melting the metal in carbon monoxide produced the  $\operatorname{Ln_2O_2C_2}$  phase, though it was demonstrated micrographically that the fused ingot had to be fractured and re-arced several times before it showed homogeneity. The carbon deposit on the hearth around the samples indicated that the reaction may have involved carbon and oxygen species formed from carbon monoxide by the very high arc temperatures.

#### 2. Analytical Results

The results of Nd<sub>2</sub>O<sub>2</sub>C<sub>2</sub> analyses performed by R. B. Leonard are reported here. <sup>22</sup> Vacuum-fusion analysis indicated that neither nitrogen nor hydrogen was present in the sample, since all the gas evolved in the vacuum fusion was found to be carbon monoxide. Similarly the gases liberated when sesquioxide reacted with graphite were found by use of the mass spectrometer to consist of greater

than 99% carbon monoxide, with 0.3%  $\rm H_2$  , 0.1%  $\rm N_2$  and traces of other species.

Mass spectrometric analyses of the gas samples removed from the system during equilibration studies of  $\text{La}_2\text{O}_2\text{C}_2$  indicate the following:

$$H_2$$
, 1.02 ± 0.5%

$$0_2$$
, 1.38 ± 0.7%

These data indicate that the reversible pressures measured during equilibration experiments were within 2% of the true carbon monoxide pressure, and the pressure and temperature data recorded did indeed represent a series of equilibrium states.

The percentages determined from 20 analyses performed on seven different neodymium oxycarbide preparations are as follows:

$$c, 6.3 \pm 0.9\%$$

0, 
$$10.8 \pm 1.1$$
 (difference)%

$$8.43 \pm 0.21 \text{ (fusion)}\%$$

The carbon content was considered a minimum value since the sample was always exposed very briefly to air. These data, when reduced to molar ratios, determine a stoichi-ometry of

$$^{\text{Nd}}$$
1.00 ± .01  $^{\text{O}}$ 1.04 ± 0.12  $^{\text{C}}$ 0.91 ± 0.13.

based on the average of both fusion and difference oxygen analyses. These data are judged reasonably consistent with the composition NdOC.

The percentages determined from 12 metal and free carbon analyses and six total carbon analyses on the analogous lanthanum species are:

The improved standard deviations probably result from refinement of the preparatory technique by use of the arc melter. Reduced to molar ratios, these data determine a stoichiometry of

$$^{\text{La}}_{1.00} \pm .01$$
  $^{\text{O}}_{0.95} \pm .06$   $^{\text{C}}_{1.04} \pm 0.12$ .

These data are again judged reasonably consistent with the stoichiometry LaOC.

#### 3. Hydrolysis Results

The graphic display of the chromatagraphic analysis of the gaseous hydrolysis products of the neodymium species indicated acetylene, ethene and ethane

to be present. The relative peak heights (acetylene: ethene: ethane) were 945:8:5. The gaseous hydrolysis products of LaOC consisted of 96.3% acetylene, 4.1% mixed ethane-type hydrocarbons and no methane.

The LnOC phases hydrolyze very rapidly in the presence of even small amounts of water vapor, thus all manipulations had to be carried out to exclude as much atmospheric moisture as possible. Samples could not be kept uncovered in the glove box for more than one day without noticeable decomposition. Whenever possible, they were stored in a vacuum desiccator or in small paraffin-sealed vials which were kept in the glove box prior to use.

The predominance of acetylene in the gaseous hydrolysis products and the rapid hydrolytic behavior indicate that the carbon is present in the oxycarbide as  $C_2^{=}$  ions. Based on this, the formula should be written  $\operatorname{Ln}_2 O_2 C_2$  rather than LnOC.

# 4. X-Ray Diffraction Results

The principal interplanar <u>d</u>-values and the relative intensities of their corresponding lines in the x-ray diffraction patterns are listed for  $\mathrm{Nd}_2\mathrm{O}_2\mathrm{C}_2$  and  $\mathrm{La}_2\mathrm{O}_2\mathrm{C}_2$  in tables (I) and (II) respectively. The  $\mathrm{Nd}_2\mathrm{O}_2\mathrm{C}_2$  <u>d</u>-values were determined from two independently prepared samples, and the  $\mathrm{La}_2\mathrm{O}_2\mathrm{C}_2$  <u>d</u>-values are representative of four independently-prepared samples, two of which were examined

TABLE I  ${\tt OBSERVED} \ \, {\tt Nd}_2 {\tt O}_2 {\tt C}_2 \ \, {\tt X-RAY} \ \, {\tt POWDER} \ \, {\tt DIFFRACTION} \ \, {\tt DATA}$ 

Ī	d, A	Ī	o d, A
w	7.04	w	1.655
m	3.55	VW	1.623
w,m	3.42	VVW	1.607
vw	3.36	VW	1.586
vs	3.11	w	1.554
s	2.968	W	1.540
w	2.600	VW	1.496
m	2.370	vvw	1.467
m	1.989	vvw	1.452
m	1.968	VW	1.425
w	1.926	W	1.342
vw	1.890	vvw	1.322
W	1.859	vvw	1.305
vvw	1.793	vw	1.295
vvw	1.744	VW	1.282
vw	1.701	vvw	1.268
vvw	1.680	m	1.257

TABLE II  $\text{OBSERVED } \text{La}_2 \text{O}_2 \text{C}_2 \text{ X-RAY POWDER DIFFRACTION DATA}$ 

Ī	<u>d</u> , Å	Ī	d, Å	Ī	<u>d</u> , Å
m	7.30	VVW	1.834	VW	1.233
vvw	5.16	s	1.748	mw	1.209
m	3.65	W	1.705	VW	1.184
mw	3.53	VW	1.669	VVW	1.156
vw	3.479	VW	1.651	mw	1.089
vw	3.356	VW	1.638	VVW	1.066
vvs	3.172	VW	1.620	VVW	1.014
s	3.042	VW	1.594	W	0.859
ms	2.958	VW	1.577		
vw	2.613	VW	1.533		
vw	2.446	VW	1.491		
vw	2.412	VW	1.455		
w	2.269	VVW	1.403		
w	2.025	VW	1.378		
vw	1.992	VVW	1.362		
vvw	1.962	W	1.286		
vvw	1.908	W	1.258		

by the Debye-Scherrer technique and the other two by diffractometry. The precision of these <u>d</u>-values is estimated to be  $\pm$  0.01 Å. A tentative indexing based on Weissenberg photographs of a poor-quality single crystal of  $\text{La}_2\text{O}_2\text{C}_2$  indicates monoclinic or lower symmetry. (Appendix III)

## 5. Infrared Results

The infrared spectrum was virtually featureless, with no peaks in the carbonyl region (2000 cm $^{-1}$ ) or in the acetylide region (2200 cm $^{-1}$ ). One very faint peak which was observed in the 700 cm $^{-1}$  region could be attributed to a  $\equiv$ C-H rocking mode from the acetylene which was present in small quantities since the KBr sample disc was exposed to atmospheric moisture during the infrared scan.

# 6. Equilibrium Results

Three or more sets of equilibrium data were taken, with a minimum of eight pressure and temperature-defined equilibrium points in each data set. X-ray diffraction analysis of the solid phases involved in the equilibrium and mass spectrometric analysis of the gas phase indicated the equation describing the equilibrium to be

 $\operatorname{Ln_2O_3(s)} + 3\operatorname{C(s)} \stackrel{\longleftarrow}{\to} \operatorname{Ln_2O_2C_2(s)} + \operatorname{CO(g)}.$  (30) This equilibrium could not be reversed completely to the left when the starting material was arc-melt prepared  $\operatorname{Ln_2O_2C_2(s)}$  nor could it be forced completely to the right

once the equilibrium was established. These observations are apparently a result of a rapid decrease in reaction rate after a certain fraction of the material has reacted. This initial reaction probably formed a protective layer through which the carbon monoxide was absorbed or evolved only very slowly. The fraction of material which had reacted could be monitored by measuring pressure changes resulting from the uptake or evolution of carbon monoxide since the volume of the system had been calibrated previously. The effective temperature value used in the gas equation to calculate the amount of gas absorbed or evolved was determined by adding a known amount of carbon monoxide at room temperature to the system containing an empty graphite crucible. The crucible was heated and the pressure of the known amount of gas was measured as a function of crucible temperature. From this the "effective gas temperature" was determined over a range of crucible temperatures. It was found that this "effective gas temperature" changed very little for a given crucible temperature when varying amounts of gas were present in the system.

The equilibrium data were taken over a temperature range of about 1325° - 1850°. Below 1325° the reaction preceded at so slow a rate that attainment of equilibrium was difficult, and at about 1850° the powdered solid

mixture began to fuse, producing a fused layer on the sample that apparently reduced the surface area enough to drastically limit the absorption of gas. Above 1850°, the sample would completely fuse and react with the crucible with an accompanying drastic increase in carbon monoxide pressure. The fused material, which appeared to erode through the crucible, exhibited a lanthanide dicarbide diffraction pattern and was probably a eutectic of LnC2 and graphite. Although G. L. Buchel in his thesis reproted measurements of pressures over predominantly oxide samples at temperatures in excess of 2000°, the writer was unable to repeat this work using La<sub>2</sub>O<sub>2</sub>C<sub>2</sub>, and it appears that another equilibrium system was being studied above 1850°; since a change in slope occurs in the graph representing G. L. Buchel's equilibrium data at this temperature.

After a prolonged (more than 48 hours) equilibration study, small amounts of sesquioxide were always found on the graphite crucible wall exterior, and the graphite wall was pitted under sesquioxide. It appears that the lanthanide metal migrated through the graphite, possibly in the form of an oxycarbide. When the migrating phase reached the exterior wall surface (which was always a little cooler than the interior of the crucible), the carbon monoxide pressure exceeded the equilibrium value

for the phase and converted that phase to the sesquioxide and graphite. The metal was probably not present as a dicarbide phase during transport through the wall since attempts to react  $\operatorname{LnC}_2$  with carbon monoxide to form either the  $\operatorname{Ln}_2O_2C_2$  or  $\operatorname{Ln}_2O_3$  were unsuccessful. Only very small amounts of carbon monoxide were absorbed in such experiments, since a fused layer was always formed on the dicarbide when it was heated to temperatures at which the small amounts of CO were absorbed. The absorbed layer inhibited further reaction.

To prevent this exterior wall phenomenon from competing for the available carbon monoxide, a double wall crucible (Fig. 3) which eliminated the problem was devised, presumably since the crucible interior was maintained at a constant temperature over its entire surface.

Graphs of the equilibrium data for the reactions

$$Nd_2O_3(s) + 3C(s) = Nd_2O_2C_2(s) + CO(g)$$
 (31)

$$La_2O_3(s) + 3C(s) \stackrel{\leftarrow}{\rightarrow} La_2O_2C_2(s) + CO(g)$$
 (32)

are displayed in Figs. (4) and (5). The decreased scatter in the equilibrium data for  $\text{La}_2\text{O}_2\text{C}_2$  is attributed to the improved temperature control described previously

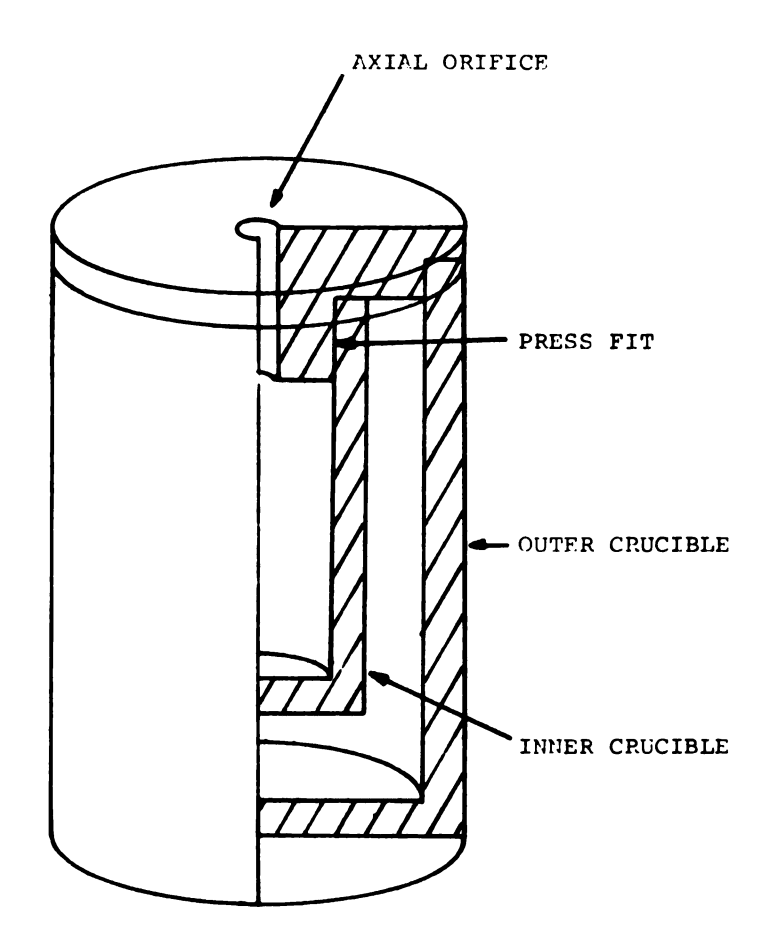
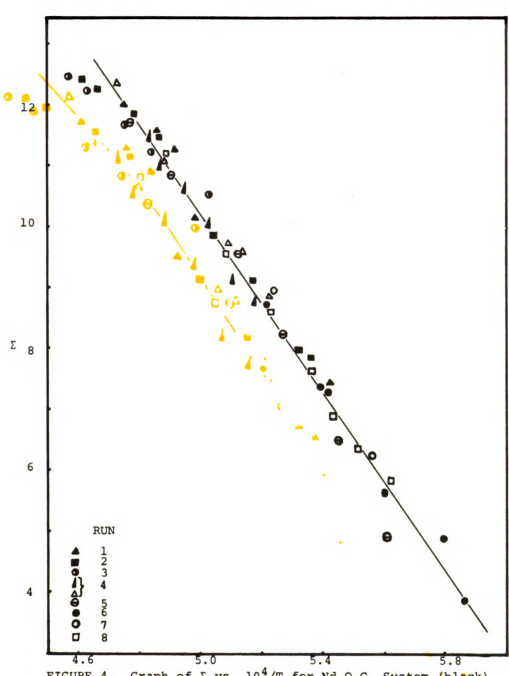


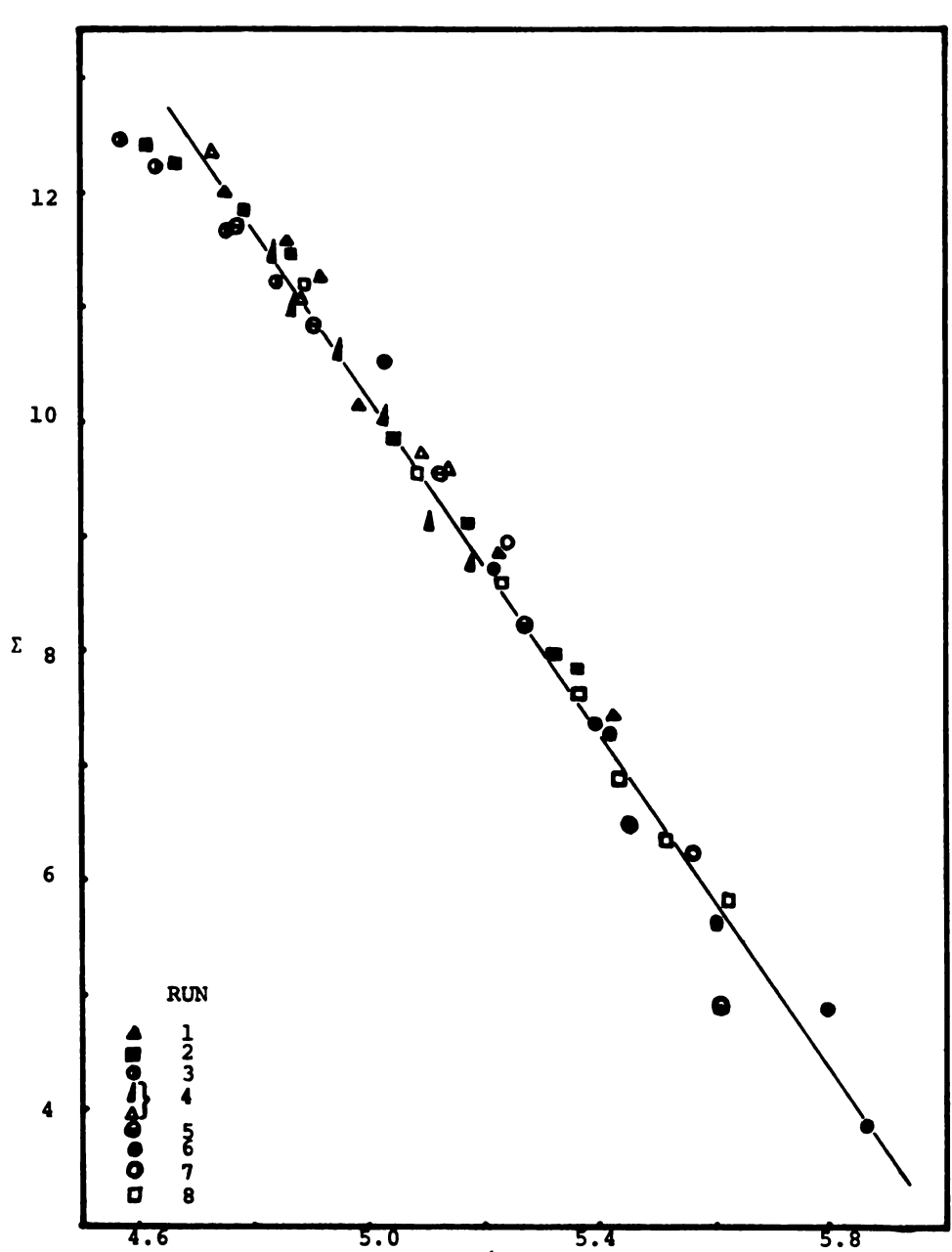
FIGURE 3. Double-Walled Graphite Crucible



5.0 5.4 5.8

FIGURE 4. Graph of E vs. 10<sup>4</sup>/T for Ma2O<sub>2</sub>C<sub>2</sub> System (black).

Overlay Shows Same Data Plotted as log P<sub>CO</sub> (atm.) in Equilibrium with Nd<sub>2</sub>O<sub>2</sub>(s), C(s), and Nd<sub>2</sub>O<sub>2</sub>C<sub>2</sub>(s) versus 10<sup>4</sup>/T



4.6

5.0

5.4

5.8

FIGURE 4. Graph of E vs. 104/T for Nd<sub>2</sub>O<sub>2</sub>C<sub>2</sub> System (black).

Overlay Shows Same Data Plotted as log P<sub>CO</sub> (atm.)

in Equilibrium with Nd<sub>2</sub>O<sub>3</sub>(s), C(s), and Nd<sub>2</sub>O<sub>2</sub>C<sub>2</sub>(s)

Versus 104/T

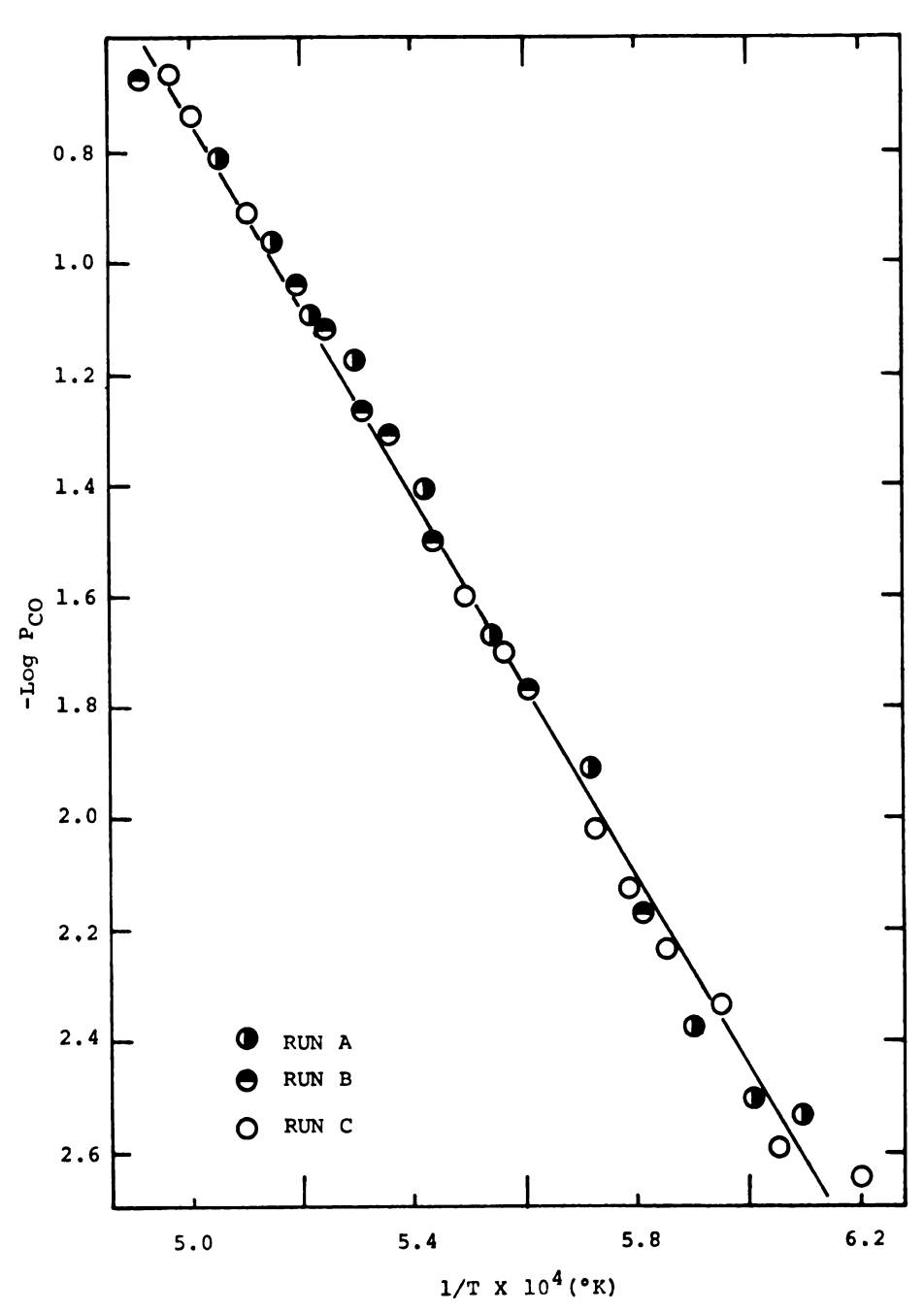


FIGURE 5. Pressure of CO in Equilibrium with  ${\tt La}_2{\tt O}_2{\tt C}_2(s)$  , C (s), and  ${\tt La}_2{\tt C}_3(s)$ 

The graph of equilibrium data measured for the  $\mathrm{Nd_2O_2C_2}$  system appeared to possess a slight negative curvature and hence was subjected to a so-called  $\Sigma$ -plot treatment, in which the  $\Delta C_{\rm p}$  for the oxycarbide was assumed constant over the temperature range of interest. The heat capacity of the oxycarbide was assumed to be that of the sesquioxide plus 7.5 cal/deg.-mole, the latter figure being three fourths of the extrapolated heat capacity differences between CaO and CaC, at 1750°. From a combination of this value with the heat capacities for  $Nd_2O_3$ , C and CO,  $\Lambda C_p$  was estimated to be -1.7 cal/ deg-mole. At a reference temperature of 1750° with a constant  $\Delta C_p$ , the function  $\Sigma$ , defined as  $\Sigma$  = R  $\ln P_{CO}$  $-\Lambda C_{p}(\ln T + 1750/T)$ , was graphed against  $10^{4}/T$  (Fig. 4). Data series 1 - 3 were made in the original apparatus (cf, page 25) with a starting mixture of  $Nd_2O_3$  and graphite, while series 4 - 8 were made in the second apparatus (cf. App. II) with starting mixtures of Nd<sub>2</sub>O<sub>2</sub>C<sub>2</sub> and sesquioxide, or only Nd<sub>2</sub>O<sub>2</sub>C<sub>2</sub>. A different specimen was used in each series. The arc-melted sample of  $Nd_2O_2C_2$  absorbed and evolved carbon monoxide quite rapidly as long as not more than 15-20 mole percent of the charge had reacted with carbon monoxide. When more than 20 mole percent of the charge had reacted, the retardation of the pressure restoration rate after a pressure excursion from the equilibrium value was probably due to the necessity for the CO to diffuse through a thick layer of solid material to reach the reaction interface.

The linear least-squares equation which describes the equilibrium data for the  $Nd_2O_2C_2$  system in the temperature region 1350 - 1850° is

$$\sum = \frac{-(72.7 \pm 1.3)}{T} \times 10^3 + (46.60 \pm 0.68)$$
 (33)

From this equation, the following thermodynamic data are calculated for reaction (31):

$$\Delta H^{\circ}_{1750^{\circ}K} = 72.7 \pm 1.3 \text{ kcal/gfw};$$

$$\Delta S^{\circ}_{1750^{\circ}K} = 32._{2} \pm 4._{3} \text{ eu.}$$

The standard deviation reported for the enthalpy represents only the scatter in the data; that reported for the entropy includes an estimated error of  $\pm$  0.5 cal/deg-mole in the heat capacity.

These data can be converted to those which represent the equilibrium system at 298° by making use of the tabulated enthalpy and entropy data for the sesquioxide, graphite, and carbon monoxide,  $^{23,24}$  and by estimating the enthalpy of the  $Nd_2O_2C_2$  to equal that

of the sesquioxide plus three-fourths the difference between the enthalpy values for CaC<sub>2</sub> and CaO. From these calculations,

$$^{\text{AH}^{\circ}}_{298}$$
 (second law) =  $75._9 \pm 3._0 \text{ kcal/gfw}$   
 $^{\text{S}^{\circ}}_{298} = 33._3 \pm 4._4 \text{ eu.}$ 

The indicated errors are estimated from those listed previously for the 1750° data, since the heat capacity correction for the oxycarbide is an estimate and thus will increase the error in the 298° K data.

The graphic display of equilibrium data describing the  $\text{La}_2\text{O}_2\text{C}_2$  system appeared to have no discernible curvature and its treatment by the  $\Sigma$ -plot method, using approximations similar to those described for the  $\text{Nd}_2\text{O}_2\text{C}_2$  data reduction, produced changes in the linear equation which were within the standard deviations computed assuming  $\Lambda\text{C}_P$  = zero over the temperature range. Thus the  $\Sigma$ -plot treatment was not applied. The set of measured data points is described by the linear least squares equation

$$\ln P_{co} = \frac{-(79.6 \pm 1.0) \times 10^3}{T} + (36.6 \pm 3.5),$$
 (34)

whose constants represent the equilibrium state of 1809°K, the mean temperature.

From this equation the following thermodynamic data may be deduced:

$$^{\text{AH}^{\circ}}_{1809} = 79.6 \pm 1.0 \text{ kcal/}_{gfw}$$
  
 $^{\text{AS}^{\circ}}_{1809} = 36.6 \pm 3.5 \text{ eu.}$ 

Heat capacity corrections similar to those applied to the previous data were used to correct these values to 298°K. The corrected data are:

$$^{\text{AH}^{\circ}}_{298} = 82.2 \pm 1.9 \text{ kcal/gfw}$$
  
 $^{\text{S}^{\circ}}_{298} = 37.7 \pm 3.6 \text{ eu.}$ 

These data show increased errors over the  $1809^{\circ}K$  data due to approximations used in determining the heat capacity of  $\text{La}_2\text{O}_2\text{C}_2(s)$ , and the reported errors in the tabulated heat capacities used for the other components of the equilibrium.

As a check on these second-law enthalpy determinations, third-law values were calculated using tabulated data cited previously for the free energy functions of  $\mathrm{Nd_2O_2C_2}$  and  $\mathrm{La_2O_2C_2}$ . The free energy function of the oxycarbides were assumed to be twice the sum of the free energy functions of the lanthanide metal, graphite, and an estimated free energy function of oxygen, whose contribution was assumed to be the difference between the free energy functions of CaO and Ca over the temperature range.

The third-law enthalpies show no significant trends over the temperature range studied, and their mean values, together with their standard deviations are:

$$\Delta H_{298}$$
 (Nd<sub>2</sub>0<sub>2</sub>C<sub>2</sub>, 3rd law) = 84.4<sub>6</sub> ± 0.6<sub>3</sub> kcal/gfw

$$\Lambda H_{298} (La_2 O_2 C_2, 3rd law) = 80.8_9 \pm 0.7_1 kcal/gfw$$

The listed errors represent standard deviations of the values rather than actual errors in the enthalpies. The agreement of the second and third-law data will be discussed subsequently. In further calculations the second-law value will be assumed correct because of the approximations used in the third-law determinations.

Combination of these second-law values with the enthalpies and free energies of formation of  $\mathrm{Nd}_2\mathrm{O}_3(s)$ ,  $\mathrm{La}_2\mathrm{O}_3(s)$ ,  $^{23}$  and  $\mathrm{CO}(g)$ ,  $^{24}$  permits calculation of the following enthalpies of formation of  $\mathrm{Nd}_2\mathrm{O}_2\mathrm{C}_2(s)$  and  $\mathrm{La}_2\mathrm{O}_2\mathrm{C}_2(s)$  at 298°F:

$$^{\text{AH}}_{\mathbf{f}}$$
 (Nd<sub>2</sub>O<sub>2</sub>C<sub>2</sub>(s)) = 329 ± 3 Kcal/<sub>gfw</sub>

$$\Lambda H_{\mathbf{f}}^{\circ} (La_2 O_2 C_2(s)) = 320 \pm 2 \text{ kcal/gfw}$$

and similarly the free energies of formation at 298°K are:

$$\Delta G_f^{\circ} (Nd_2O_2C_2(s)) = 309._9 \pm 3._9 \text{ kcal/gfw}$$

$$\Lambda G_{f}^{\circ} (La_{2}O_{2}C_{2}(s)) = 315.6 \pm 2.9 \text{ kcal/gfw}.$$

The reported deviations represent the accumulated errors resulting from the arithmetic manipulations on the standard deviations of both the measured and published data.

# E. Ln<sub>2</sub>0<sub>2</sub>c<sub>2</sub> PHASE, CONCLUSIONS AND DISCUSSION

## 1. General Discussion

#### a. Stoichiometry and Bonding

The stoichiometry of this phase, determined to be  $\operatorname{Ln_2O_2C_2}$ , is of interest not only because of its support of the model proposed in the introduction, but also because of its implications.

First, the stoichiometry does in fact appear to support the exchange of an oxide ion for an acetylide ion, and can be considered the result of the operational process

$$\operatorname{Ln}_{2} \circ_{3}(s) + c_{2}^{=} \rightarrow \operatorname{Ln}_{2} \circ_{2} c_{2}(s) + o^{=}.$$
 (35)

Second, the stoichiometry implies the formal oxidation state of the lanthanide metal is tripositive. This implication is somewhat unexpected as acetylide and methanide ions have normally been seen to stabilize low formal oxidation states for the lanthanides by facilitating the formation of conduction bands which accept valence electrons from the tripositive lanthanide ions. That this apparently does not happen may be due to one or both of the following postulates:

- (a) the acetylide ions are "diluted" by the oxide ions, and their effect is thus nullified.
- (b) the symmetry of the acetylide sites is such that whatever combination or overlap of ionic orbitals is needed to form conduction bands is effectively prevented.

The first postulate is thought the less probable, since the phases discussed in the following chapters possess O/C ratios of three to one, yet are excellent conductors. A strict comparison is not valid, however, because of the different nature of the carbon units.

Conductivity measurements were not performed on this phase, since small amounts of graphite were always present in the preparations. The appearance of small transparent crystals of  $\text{La}_2\text{O}_2\text{C}_2$ , used in the Weissenberg technique, does support the non-existence of conduction bands in these phases, as metallic conductors normally exhibit opaque crystals with varying degrees of metallic color (description of Weissenberg experiments in Appendix III).

The hydrolysis behavior reveals much about the bonding and the ionic species in the crystal. The appearance of no hydrolysis products other than acetylene is indicative of two facts:

- 1. All bound carbon present in the  ${\rm Ln_2O_2C_2}$  phase is in the form of acetylide ions, as any methanide units would produce appreciable quantities of methane. This information indicated the correct formula to be  ${\rm Ln_2O_2C_2}$  rather than the empirical LnOC formula, also consistent with the analytical results.
- 2. The complete absence of higher molecular weight hydrocarbons indicates that no oxidation or reduction occurred during the hydrolysis. If any of the metal were in the Ln<sup>+2</sup> oxidation state, it would reduce some of the acetylene, and would form higher molecular weight hydrocarbons. The metal is thus deduced to be in the tripositive state in the crystal.

The rapidity of the hydrolysis has been considered to be an indication of the ionic character of the metal-carbide bond. <sup>27</sup> By this criterion, the  $\rm Ln-C_2$  bond is very ionic, since the hydrolysis of  $\rm Ln_2O_2C_2$  occurred with extreme rapidity in even very small amounts of atmospheric moisture.

From the preceding arguments, it is apparent that the  $\operatorname{Ln_2O_2C_2}$  phase is a crystalline material of highly ionic character, consisting of tripositive lanthanide cations, oxide and acetylide anions. The phase can be considered as a lanthanide sesquioxide

lattice with one-third of the oxide ions replaced by acetylide ions.

#### b. Structure

If one were able to replace (as proposed in the preceding model) one-third of the spherical oxide ions in a sesquioxide lattice by acetylide ions, the resultant species would undoubtedly be a distortion of the parent oxide lattice, since the  $C_2^{=}$  ion is markedly anisotropic. Though the average C-C bond distance in the lanthanide dicarbides is 1.285  ${\rm \mathring{A}}^{28}$  and the radius of the oxide anion in metal oxides is of the order of 1.3 A, the actual space filled by the acetylide ion is evidently much greater. This can be demonstrated by comparing the lattice parameters of the cubic forms of CaO and CaC, which are 4.799 Å and 5.393 Å respectively. 29 The difference is about 0.6 A. This comparison, however, assumes the two sites to be equivalently spherical. addition to this size difference, the oxide ion is spherical while the acetylide ion possesses a prolate shape. A determination of the relative anisotropy of the acetylide ion can be made by comparing the lattice parameters (a = 5.49 Å, c = 6.38 Å)<sup>29</sup> of the tetragonal CaC, unit cell. The difference in length is due only to

the orientation of the acetylide unit, therefore, one can conclude that the space occupied by the anistropic  $C_2^=$  unit is about 0.5 Å greater in one dimension than the other. The  $CaC_2$  was selected for this comparison rather than some lanthanide dicarbide since the calcium undergoes no apparent formal oxidation state change upon  $C_2^- \longleftrightarrow 0^-$  substitution and is comparable in size/charge ratio to  $La^{+3}$ . It may be that the  $C_2^-$  unit changes in dimensions with conduction band formation in the  $LnC_2$  structures, since the c-a difference for their unit cell dimensions is of the order of 2.3 Å.  $^{29}$ 

The combination of the size increase of the acetylide ion over that of the oxide and the prolate shape of the acetylide unit probably render impossible any estimates concerning the effect of the model (acetylide-for-oxide) substitution on the oxide structure, but certainly would lead one to suspect that the structure possesses fairly low symmetry compared to the sesquioxide or dicarbide. The probable monoclinic cell indexing presented in Appendix III is consistent with these observations.

An oxycarbide phase purported to be LnOC (Ln = La, Ce, Nd, Sm, Gd) has been indexed on the basis of a monoclinic cell by Leprince-Ringuet. 30 Comparison

of the <u>d</u>-values expected from their reported unit cell for LaOC with the measured <u>d</u>-values for the lanthanum phase reported in this work shows that the  $\text{La}_2\text{O}_2\text{C}_2$  is probably indexed incorrectly, since too many diffraction lines corresponding to <u>d</u>-values predicted by their unit cell are not found in the  $\text{La}_2\text{O}_2\text{C}_2$  diffraction pattern.

Other comparisons with the French work are of interest. They report the isostructural analogues of this LnOC phase for samarium, cerium, and gadolinium, in addition to neodymium and lanthanum. Attempts in this laboratory to prepare the samarium and gadolinium analogues of  $\text{La}_2\text{O}_2\text{C}_2$  and  $\text{Nd}_2\text{O}_2\text{C}_2$  failed. The cerium-oxygen-carbon system might be of interest, since one would anticipate the acetylide-oxygen substitution would take place in the cerium dioxide, rather than the sesquioxide system, though the acetylide units might stabilize the lower tripositive oxidation state of cerium.

The inability to form the  $Sm_2O_2C_2$  and  $Gd_2O_2C_2$  could possibly be explained in two ways:

1. The ionic radius change in the lanthanide metal between neodymium and samarium might be sufficient to destabilize the  ${\rm Ln_2O_2C_2}$  phase which exists for the lighter lanthanides. Surely this is the principal difference between neodymium and samarium compounds with oxygen and carbon.

2. Samarium shows some stability in the dipositive state, and the carbon might be able to promote conduction-band formation, and consequent phase change from the neodymium to the samarium analogue.

The apparent invariance of any lattice parameters in the  $\text{Ln}_2\text{O}_2\text{C}_2$  phase when prepared with an excess of any component is indicative of narrow composition limits. It appears that the C/O ratio is relatively fixed, a behavior quite different from other oxycarbide phases  $U(0,C)^{10,14}$  and  $Zr(0,C)^{31}$  which show variable O/C ratios. Ternary phases of Ln-O-C are also quite different from the Ln-O-N ternary phases which appear to be solid solutions of nitride and oxide of the lanthanide used and possess widely variable N/O ratios. 32,33 This seeming invariance of the C/O ratios in Ln<sub>2</sub>O<sub>2</sub>C<sub>2</sub> might be accounted for on the basis of the anisotropic shape of the acetylide ion. Apparently the acetylide ions occupy ordered lattice sites (not equivalent to the oxygen sites), and any change in the C/O ratio outside of very narrow limits varies this anionic ordering and destabilizes the lattice.

2. Relationship of La and Nd Analogues of  $\text{Ln}_2\text{O}_2\text{C}_2$ 

# a. Structure

Comparison of the x-ray diffraction patterns of  ${\rm La_2O_2C_2}$  and  ${\rm Nd_2O_2C_2}$  showed that the lines of the

two patterns corresponded on a one to one basis, with slightly smaller d-values being calculated for the Nd202C2 than La202C2. From this, it can be concluded that the phases are indeed isostructural, and the slightly smaller d-spacings for any given set of planes in the  $\mathrm{Nd_2O_2C_2}$  than the  $\mathrm{La_2O_2C_2}$  are consistent with the 0.066  $\mathrm{A}^{34}$ smaller ionic radius of Nd<sup>+3</sup>. The observed appearance of a new phase on the attempted preparation of the  $Sm_2O_2C_2$  and  $Gd_2O_2C_2$  has already been noted. diffraction patterns for the Sm(OC) and Gd(OC) are unrelated to the patterns of the  $\text{La}_2\text{O}_2\text{C}_2$  and  $\text{Nd}_2\text{O}_2\text{C}_2$ . This phase change between the oxycarbide of neodymium and samarium is paralleled by the high temperature behavior of the lanthanide sesquioxides, in that the hexagonal lattice found for the lighter lanthanides is replaced by the monoclinic lattice as the most stable high temperature form as one moves from Nd to Sm. Nothing quantitative can be stated from this comparison, but the parallelism of the oxycarbides and sesquioxides is not inconsistent with the model proposed, which is based on the sesquioxide lattice.

#### b. Thermodynamics

A comparison of the enthalpies observed for the equation (3) is of interest. For the reaction,  $\Delta {\rm H}_{298}^{\circ}$ 

changes from  $-82._2 \pm 1._9 \text{ kcal/}_{gfw}$  for Ln = lanthanum to  $-75._9$  for Ln - neodymium. Similarly, the heat of formation of the oxycarbide at 298° varies from  $-329._8 \pm 3._0$  for  $\text{Nd}_2\text{O}_2\text{C}_2$  to  $-320._0 \pm 2._0$  for  $\text{La}_2\text{O}_2\text{C}_2$ , or an increase in stability of about ten kcal/ $_{gfw}$  of the neodymium over the lanthanum analogue. This behavior again parallels the oxide system, when the increase in  $-\Delta\text{H}_f^\circ$  of the  $\text{Nd}_2\text{O}_3$  over that of the  $\text{La}_2\text{O}_3$  is about 3.6 kcal/ $_{gfw}$ .

## 3. Phase Relationships

The lack of stability of the  ${\rm Ln_2O_2C_2}$  phase in a carbon container above 1850° and yet its formation by arc melting at temperatures well in excess of 2000° indicate that eutectic formation with graphite is apparently the limiting factor in reactions studied with graphite present. A small amount of graphite, however, is always present when the system is in equilibrium at high temperature, and this presumably will complicate the equilibrium study of the system above the fusion temperature since the graphite present at those temperatures will undoubtedly form a eutectic. This eutectic apparently has a much higher equilibrium pressure of carbon monoxide than the pure  ${\rm Ln_2O_2C_2}$  for a given temperature and thus forms the  ${\rm LnC_2}$ .

# CHAPTER III. Ln<sub>4</sub>0<sub>3</sub>C PHASE

#### A. INTRODUCTION

In an attempt to prepare phase analogues of  $\operatorname{La_2O_2C_2}$  and  $\operatorname{Nd_2O_2C_2}$ , the methods of the previous chapter were applied to the samarium, gadolinium, holmium, and erbium systems. In all systems the attempt failed and a new phase appeared. This new phase forms the basis for the work reported in the second half of this thesis.

#### B. EXPERIMENTAL METHODS

#### 1. Preparation

This phase was first prepared by arc melting a pressed pellet of a lanthanide metal heavier than neodymium, its sesquioxide, and graphite in the molar ratios (Ln:0:C) of 1:1:1 under 1.1 - 1.2 atmospheres of CO. As has been noted, this preparation was carried out in an attempt to prepare the heavier lanthanide analogues the  $\operatorname{Ln_2O_2C_2}$  phases, and the procedure used in the arc melt technique was identical with that discussed in Chapter (II).

The samples prepared by the technique described previously were shown by x-ray diffraction to contain no  $\operatorname{Ln_2O_2C_2}$  (or so little as to be undetectable by this method). Instead, the samples exhibited the diffraction patterns characteristic of two different phases:

- (1) the readily-identified sesquioxide of the lanthanide metal
- (2) a new phase of apparent cubic symmetry, which could not be indexed on the basis of any known oxide or carbide of that particular lanthanide.

The first objective in the study of this phase was its preparation in a state of purity adequate for

analysis. In an attempt to eliminate the sesquioxide impurity, the  $\text{Ln}_2\text{O}_3/\text{Ln}$  ratio was decreased by one half. The resulting x-ray diffraction pattern was almost identical with that of the previous preparation, but micrographic examination of the arc-melted ingot showed small amounts of the metal. On the assumption that this cubic phase was some oxycarbide which was in equilibrium with carbon monoxide, carbon and sesquioxide at high temperatures, the reduction of carbon monoxide pressure during arc melting might reduce the amount of sesquioxide present by shifting the reaction equilibrium. Consequently, the partial pressure of carbon-monoxide was reduced by diluting it with helium in a 1:1 ratio. The product prepared in this manner showed a marked decrease in the intensity of the sesquioxide diffraction patter compared to that of the cubic phase, implying that a further reduction in the partial pressure of carbon monoxide might allow preparation of a pure product. The partial pressure of carbon monoxide was further reduced until the samples were arc melted in pure helium. procedure resulted in the complete disappearance of the Ln<sub>2</sub>0<sub>3</sub> diffraction pattern.

In addition to the cubic pattern, however, some other very faint lines not indexable on the basis of any

known compound of the lanthanide were now seen in the diffraction pattern. In an attempt to prepare samples free of this impurity, a series of mixtures having varying Nd/O/C molar ratios were arc melted under similar condditions. The fused ingots were examined both micrographically and by x-ray diffraction in an attempt to develop a preparatory scheme which would produce the cubic phase having the greatest phase purity. The amounts of oxygen and carbon in the sample mixtures (Ln:O:C) were varied in a systematic way by fifteen mole-percent increments over a range of 100:15:85 to 100:85:15. Another series of starting mixtures of very low carbon content (O:C of 100:0 to 85:15 in 5 mole-percent increments) was also prepared, based on the postulate that the cubic phase was a carbon stabilized monoxide of the lanthanide.

As with the previous oxycarbide phase,  $\operatorname{Ln_2O_2C_2}$ , this cubic phase hydrolyzed very rapidly in atmospheric moisture, particularly when in a finely divided state. This rapidity was demonstrated by the pyrophoric hydrolysis of the finely-divided oxycarbide spattered on the hearth of the arc melter. The hydrolysis occurred within seconds after the arc-melter was opened following the preparation of samples of the cubic phase. The larger droplets hydrolyzed more slowly and without pyrolysis. The fused

ingots were transferred into the glove box as quickly as possible after preparation and all subsequent sample preparation for x-ray diffraction or other analytical methods was accomplished in the glove box. The samples were stored in massive form either in paraffin-sealed vials in the glove box or in a vacuum desiccator, thereby minimizing the hydrolysis of the product. Unlike the  ${\rm Ln_2O_2C_2}$  phase, the cubic phase hydrolysis rate appeared to slow after an initial coat of hydrolysis products covered the surface.

Fractured pieces of the prepared samples which appeared by micrographic analyses to be the most monophasic were then annealed in a  $ZrB_2$ , TaC or graphite crucible which had been outgassed previously at temperatures of 1850° to 1900°. Annealing was accomplished by heating the sample to 1650° for not more than thirty minutes in a helium atmosphere of approximately  $10^{-2}$  torr. Small amounts of gold-colored material were found on the bottom of the crucible after the annealing procedure, though the samples themselves remained unfused.

One sample was cooled quite slowly (approximately 10° per minute) from the annealing temperature to room temperature by gradual diminuation of the furnace output.

The sample subjected to this protracted cooling was compared

by x-ray diffraction with a similar sample which had been cooled as rapidly as possible from annealing temperature by suddenly shutting off the furnace. This procedure was effected to determine if the cubic phase was a high-temperature modification quenchable by rapid cooling rather than a phase stable from room to fusion temperature.

Postulation that the gold-colored fused material observed in the annealing process was an eutectic impurity suggested that a pure, monophasic material might be prepared utilizing a zone-refinement technique.

A mechanism which allowed the electrode of the arc-melter to move laterally over a rod-shaped ingot of sample to effect a zone-refinement of the ingot was developed. (This method and the apparatus is described in Appendix IV.)

Another preparatory method was the reaction of a mixture of appropriate molar ratios in a sealed bomb. Molybdenum was chosen as the bomb container material since it was found relatively inert to both graphite and carbon monoxide at the temperatures (up to 1850°) and heating periods (three to four hours) employed. This effective inertness had been established by x-ray diffraction examination of scrapings from a molybdenum surface in

3.

7

ţ

contact with graphite for the temperature and time involved and by x-ray diffraction examination of a piece of molybdenum metal fused under carbon monoxide in the arc melter.

Since it was hoped that this could be related to the previously described work, the neodymium phase was studied initially. Neodymium, its sesquioxide and graphite in the appropriate ratios were placed in a previously outgassed molybdenum bomb, prepared by heliarcing a plug in the end of a 6.35-mm O.D. molybdenum tube about 3.5 cm long. After the bomb was loaded, it was sealed by a second plug which was heliarced to the open end of the tube. This tube was then heated to about  $1850^{\circ}$  by an induction furnace under a pressure of less than  $1 \times 10^{-5}$  torr for not more than four hours. The tube was transferred to the glove-box when cool and the fused sample removed for analysis.

A further refinement of the bomb technique involved zone-refining a sample enclosed in a tubular bomb about 8 cm long. The loaded bomb was preheated to 1850° in the induction furnace as described previously, prior to zone refining. Since the fused sample always occupied less volume than the reaction mixture, typical tube bombs were about one-third to one-half full after

induction heating. The tube bomb containing the sample to be zone-refined was placed in the zone-refiner in a position inverted with respect to the position in which it was pre-reacted. This orientation allowed any relatively low-melting impurities to be carried into the empty portion of the bomb upon zone-refining.

The apparatus used for the refining process was a MRC electron-beam zone-melter model EZB-94 (described in more detail in Appendix V). The surface temperature of the heat zone was maintained at around 1700°, which is equivalent to a correct temperature of approximately 1885° based on a spectral emissivity of 0.37. The heat zone was twice swept down the tube at a rate of 0.33 mm/min.

# 2. Analysis

# a. Metal Analysis

Samples for analysis were weighed in the glove box from a finely powdered and thoroughly mixed specimen. As with  $\operatorname{Ln_2O_2C_2}$ , a homogeneous sample was used so that combination of results from analyses using different portions of this sample was possible. The hydrolysis of the samples was carried out differently from the method used for metal analysis of the  $\operatorname{Ln_2O_2C_2}$  phase. If the HCl were added directly to the powdered sample, the

hydrolysis proceeded pyrophorically. Samples treated in this manner contained large amounts of flocculent black material in solution in contrast to solutions formed when the hydrolysis was accomplished without pyrolysis. To prevent this behavior, the tared samples were partially hydrolyzed prior to addition of the HCl. At first, water vapor from a steam source was directed on the samples to effect the pre-hydrolysis, but later the sample was treated with about 10 ml. of distilled water. The remainder of the metal analysis was accomplished exactly as described in Chapter II, by precipitating the metal as the oxalate and firing it to form the sesquioxide.

# b. Carbon Analysis

The free carbon analysis was accomplished as before, by filtering the digested solution resulting from the hydrolysis to collect the unbound carbon.

The total combustion method was employed for carbon analyses as described previously, but with the following modifications. Whereas the oxidation of all the carbon in the  ${\rm Ln_2O_2C_2}$  phases was always completed within six hours as demonstrated by the constant weight of the absorber after that time, complete oxidation of the cubic phase was accomplished far more slowly, require more than twenty-four hours. It is assumed that this very slow overall oxidation rate is due to diffusion control of the

reaction, with the oxide coating formed initially inhibiting further oxidation. This behavior paralleled the hydrolytic behavior of non-pulverized samples. long oxidations necessarily introduced unwanted error into the total carbon determinations, since the blank rate for the absorber became a significant factor for oxidations requiring more than twelve hours. The oxidation time was shortened by introducing a few ml of distilled water by a long pipette into the quartz sample boat prior to heating. The system was closed very quickly to prevent escape of any hydrolysis products and the flow of oxygen initiated, carrying hydrolysis products fromed into the oxidizer section where the hot CeO2 - CuO catalyst facilitated the oxidation to carbon dioxide and water. After about thirty minutes, the temperature of the sample was elevated. The complete oxidation of carbon, which was evidenced by the absorber attaining constant weight, was now achieved within eight hours.

Because the addition of water into the oxidation chamber would add mass to the ascarite absorber if it were not completely removed, the  $\rm H_2SO_4$  and  $\rm Mg(ClO_4)_2$  dessiccants were replaced prior to each total carbon analysis. This procedure assured the presence of a fresh  $\rm H_2O$  absorption system for each experiment.

## c. Oxygen Analysis

Oxygen analysis of the cubic phase was accomplished via the vacuum-fusion method of Gregory and Mapper, <sup>37</sup> which will be described in some detail. The apparatus used (Fig. 6) consists of four principal sections:

- (1) fusion furnace
- (2) transfer pump
- (3) volumetric analysis system
- (4) main diffusion pump with its mechanical backing pump.

The fusion furnace contains a graphite crucible in which the fusion occurs (5) and is equipped with an optical window for temperature measurement (6) and magnetically activated magazines for the addition of platinum (7) or samples (8) to the crucible. The transfer pump (2) is a mercury diffusion pump which will maintain a low pressure (of the order of 10<sup>-5</sup> torr) in the fusion furnace with relatively high backing pressures (up to 1 torr) in the volumetric analysis system. The volumetric analysis system (3) can be closed off from the main pump (4) and used for quantitative determination of gases by means of the multiple-range McCleod gauge (9). The system volume, which can be varied by valving the fixed volumes (10) in or

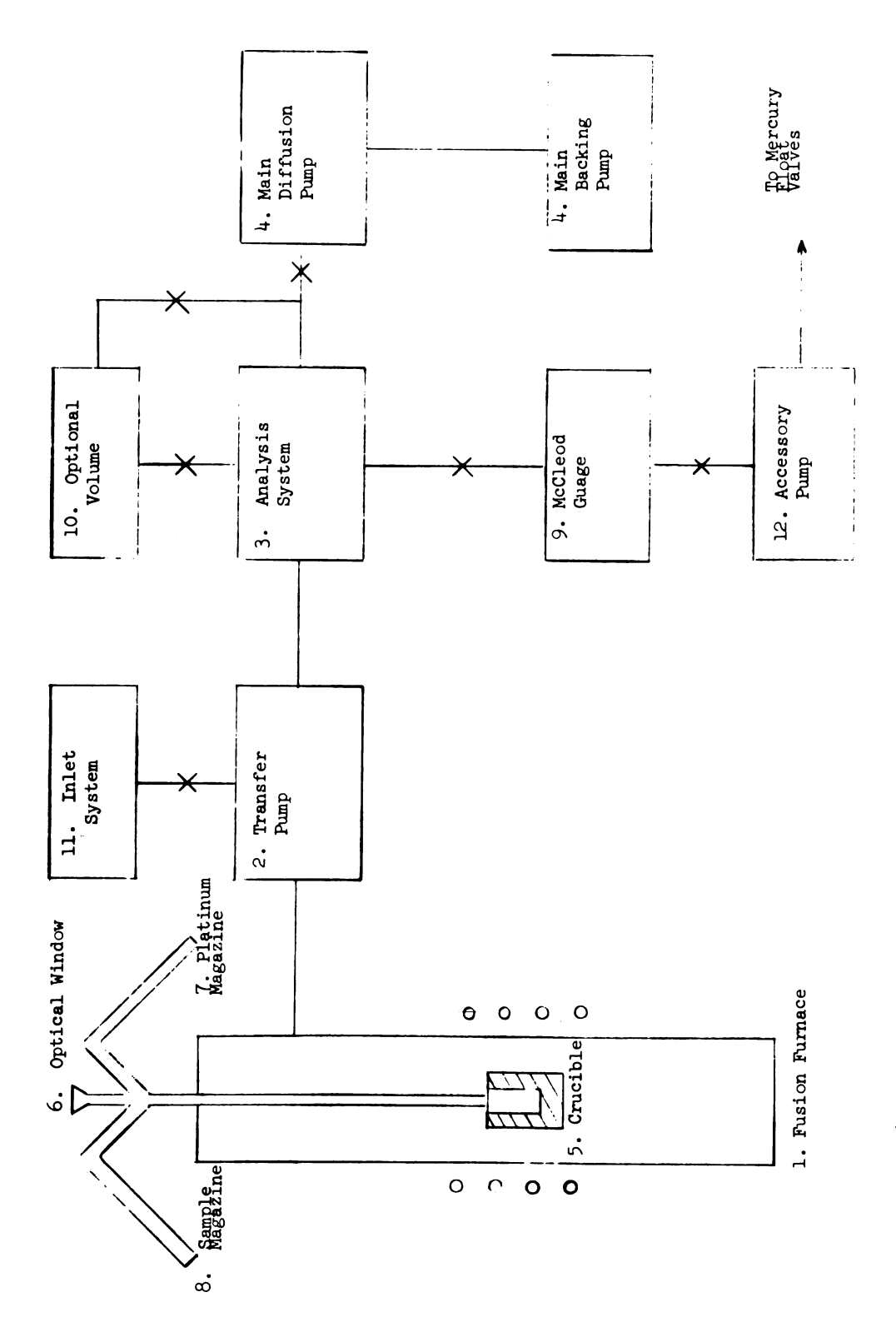


Fig. 6. Oxygen Analysis System

out of the volumetric system is calibrated by admitting known amounts of gas through the inlet (11). The main pump (4) is used to evacuate the entire system or any part of it by the proper combination of valve settings. The valves used throughout the volumetric system are mercury float valves, which prevent the contamination of the gas. The external side of the mercury float valves is evacuated by the backing pump (12) which is entirely independent of the rest of the vacuum system.

To effect the analysis, the oxygen-containing sample is dropped into a molten platinum bath confined in the graphite fusion crucible. At temperatures at or above the melting point of platinum (1770°), considerable carbon is present in the fused metal. 38 This carbon reacts with any metallic oxide, nitride, or hydride, forming either the metal or the metal carbide and evolving the particular non-metal in the form of the elemental gas for the nitride and hydride or as carbon monoxide in the case of an oxide. The quantity of the gas evolved is determined volumetrically by expanding it into the evacuated, closed analytical system whose volume is known and by noting the pressure drop in the volumetric system. By combining these pressure-volume relationships with the gas temperature data, the quantity of gas present

can be determined. Four samples of the cubic phase were prepared for oxygen analysis by weighing approximately 25 mg of pulverized sample into cup-shaped containers formed from 1 cm x 1 cm sheets of 0.13 mm thick platinum. These containers were then folded to prevent sample loss and pressed into compact, cylindrically-shaped pellets of approximately 5 mm in diameter and length in the glove The pellets were loaded into the sample magazine behind three similarly-sized samples of freshly-calcined Nd<sub>2</sub>O<sub>3</sub> which were to be a standard oxygen source to check the accuracy and reproducibility of the analysis system. From 10 to 11 g of platinum, in the form of tight rolls of platinum formed from 5 x 40 mm strips of 0.5 mm thick sheet, was placed in the platinum-bath magazine and a previously outgassed graphite fusion crucible (Ultra Carbon Corp., Bay City, Mich.) was positioned in the fusion furnace in a graphite powder bed, which serves as a support for the crucible.

The system was evacuated and both diffusion pumps turned on. When a pressure of less than  $10^{-5}$  torr was attained in the system, the crucible was heated slowly to a temperature of 2100° and outgassed at this temperature for 12 hours. At the same time, the volumetric analysis portion of the system was also outgassed, by use of heating

tapes wrapped around the glass section to reduce further the so-called "blank rate" describing the pressure stability when the volumetric analysis system was isolated from the pump. The blank rate was considered acceptable when the pressure of the volumetric system did not increase from  $10^{-6}$  torr to more than  $5 \times 10^{-4}$  torr in a fifteen minute interval from the time it was isolated from the pump. When an acceptable blank rate was achieved, the crucible temperature was decreased to about 1200°, and the analysis system was closed off from the pump and its pressure recorded. A sample was dropped into the crucible and its temperature was increased to 1800° - 1825° to effect extraction of the carbon monoxide. The pressure in the volumetric analysis system was checked periodically, and when it attained a stable value (usually within twenty minutes), the temperature was recorded. From the change in pressure upon evolution of carbon monoxide, the volume of the analysis system and the temperature of the gas (assumed identical with room temperature twenty minutes after its evolution), the amount of the carbon monoxide was determined using the ideal gas law (valid in the pressure range  $10^{-6}$  to  $10^{-1}$  torr for the two significant figure measurements made). The percentage of oxygen in the original sample is calculated from the amount of carbon monoxide formed.

## d. X-Ray Analysis

The initial identification of this cubic oxycarbide phase and most of the analytical work necessary for development of the preparatory techniques was effected by Debye-Scherrer x-ray diffraction analysis, employing cameras of 114.6 mm diameter and copper ( $\lambda\alpha_u=1.5418~\text{Å}$ ) radiation. The use of the Debye-Scherrer method in phase purity determination was facilitated by the relative ease with which the cubic pattern could be identified and the fairly good intensities of the diffraction lines, in contrast to the intensities of the sesquioxide and the  $\ln_2 \Omega_2 C_2$  patterns. Capillaries of 0.3 mm diameter for use in the cameras were filled in the glove box and flame-sealed immediately upon their removal from it.

More detailed x-ray diffraction measurements were made on Siemens and Norelco diffractometers. The powdered diffractometric specimens were mounted on glass slides by spreading evenly a very thin layer of Canada balsam-sample mixture over the center of the glass surface. When this mixture had hardened and the surface of the sample was dry, another very thin coat of the Canada balsam, diluted with xylene, was flowed over the sample surface to provide a barrier against hydrolysis by atmospheric moisture. These samples appeared to remain

unaffected by exposure to the almosphere for 4-6 hours, after which the slight change of color of the surface indicated the onset of hydrolysis. The diffractometric patterns were analyzed for faint superstructure lines which would be indicative of some ordering of lattice sites. In addition, intensity measurements on the peaks representing (111) and (002) planes in the diffractometer pattern were effected by measuring the areas subtended by those peaks with a polar planimeter.

## 3. Hydrolysis Experiments

An open, wide-mouthed vial containing a specimen of this cubic oxycarbide was placed carefully into a 500 ml. flask fitted with a side arm to which a stopcock was attached. Care was taken to insure that the vial remain upright throughout the experiment. The flask was sealed with a rubber stopper and evacuated through the side arm. Ten ml of distilled water was then added to the evacuated flask by filling an external tube leading to the stopcock, opening it carefully and letting the water enter the evacuated flask very slowly. Care was taken to insure that water did not come in contact with the sample. After two days of hydrolysis, helium was admitted to bring the internal gas pressure up to about one

atmosphere. Gas samples of the contents were withdrawn with a syringe inserted through the rubber stopper, and subjected to gas chromatographic analysis in an F and M model 810 gas chromatograph, which utilized six foot columns filled with 100-120 mesh Porapack Q (Waters Assoc., Inc., Framingham, Mass.). Flame ionization detectors were used. Retention times had been calibrated by use of samples of CP methane or CP acetylene.

#### 4. Equilibrium Studies

Attempts were made to determine if this phase formed a component in any equilibrium systems involving carbon monoxide, and was thus possibly suitable for study by the same methods used in the  ${\rm Ln_2O_2C_2}$  equilibrium measurements.

# RESULTS, Ln<sub>4</sub>0<sub>3</sub>C PHASE

# 1. Preparatory Results

The mole ratios of Nd<sub>2</sub>0<sub>3</sub>:Nd:C which yielded an arc-melted ingot judged on the basis of micrographic and x-ray diffractometric analysis to possess the highest phase purity was 1:2.5:1, and the metal:oxygen:carbon ratios were 4.5:3:1. Very little quantitative information can be deduced from these starting ratios, however, since considerable amounts of carbon were deposited on the hearth around each sample (along with small pieces of the sample spattered there by the arc), and a thin layer of sesquioxide was usually found on the interior surfaces of the arc-melter chamber.

Micrographic examination of this "best" sample prepared according to ratios indicated above showed small amounts of a gold-colored minor phase distributed through the gray-silver major phase. The "herringbone" pattern exhibited by this minor phase indicated that it was probably the lower melting of the two components, and the annealing experiments were not only used to sharpen

the x-ray diffraction pattern by allowing quenched-out crystal disorders to be relieved, but also as an attempt to melt this minor phase and hopefully to remove at least part of it from the major phase.

That this indeed occurred was demonstrated by the micrographic analysis of the samples after annealing. "Herringbone" shaped voids, which were similar in size and shape to the patterns shown by the minor phase prior to annealing, appeared in the unfused major phase. The identity of the minor phase could not be determined definitely, however. It appeared that the fused material in the crucibles after annealing was an eutectic of NdC2, but it might have been a different phase which was converted to an NdC2 eutectic after exiting from the major phase. The identification of small amounts of impurity phases often presents a formidable problem.

Attempts to prepare samples of greater apparent phase purity by using the arc-melter as a zone-refiner (Appendix IV) failed. However, larger amounts of sesquioxide were found on the interior of the arc melter after an attempt at zone refining than after a normal preparation.

The unfused major phase after annealing exhibited very small amounts of the minor phase, usually in the portion

of the sample which was in contact with the bottom of the crucible. Consequently, these materials were judged to be sufficiently monophasic for analysis.

approximate stoichiometry of "Nd<sub>3</sub>O<sub>2</sub>C." It was apparent that if some preparative technique were devised in which no material was lost from the sample, the above stoichiometry could be checked independently by preparing a sample according to its indicated mole ratios, then analyzing the phase purity of the product.

Since molybdenum does not react measurably with carbon monoxide (an anticipated decomposition product of any oxycarbide) and only very slightly with carbon at the temperature and reaction times employed, a sample in the above ratio was sealed in a molybdenum bomb and heated.

Preparations based on the postulated "Nd<sub>3</sub>O<sub>2</sub>C" reactant ratio were found by micrographic analysis to have very small amounts of the gold-colored minor phase present. However, the ability to confine the phase to a sealed bomb did suggest use of a zone refining technique.

The zone-refinement technique described in the previous chapter proved successful. Small amounts of

material were separated from the sample by the zone refining and were shown micrographically to contain appreciable quantities of the gold-colored minor phase in some of the cubic phase. The amounts were still too small for x-ray diffraction identification, however. The remaining sample exhibited no minor phase upon micrography, but, curiously, still possessed small voids.

Specimens prepared in this manner were used for the oxygen analysis; much of the carbon analysis, and all of the diffractometric investigations.

# 2. Analytical Results

The analytical results, reported as weight percentages and including the standard deviations of the measurements are as follows:

Nd, 
$$90.5_0 \pm 0.2_3\%$$
  
0,  $7.9_0 \pm 0.02\%$   
C,  $1.8_2 \pm 0.7\%$ 

These data indicate a stoichiometry of

$$^{\text{Nd}}$$
1.00 ± .02  $^{\text{O}}$ 0.787 ± .002  $^{\text{C}}$ 0.24 ± 0.08

or approximately  $Nd_4O_3C$ .

### 3. X-Ray Powder Diffraction Analysis Results

The diffractometer diffraction patterns exhibited only peaks which were assignable to a face centered cubic symmetry. No indication of any superstructure was found. This lack of superstructure implies:

- either a lack of, or a statistical distribution of, lattice vacancies, or
- 2. a probable lack of ordering of the carbon sites.

The ratio of the measured intensities of the (111) and (002) peaks was compared with the values calculated for this ratio for both an NaCl and ZnS lattice type by assuming that an  $\mathrm{Nd}^{+3}$  ion and an oxygen atom located at the respective lattice sites approximate the electron density of the  $\mathrm{Nd_40_3}$ C species. The scattering factors reported by Cromer and Waber <sup>39</sup> were used for these calculations. The temperature factor of oxygen was assumed to be 1.5  $^{2}$  and that of neodymium 0.6  $^{2}$ , and the absorption correction was considered to be negligible. The complete set of calculated results (Appendix VI) shows that the differences in relative intensities between the two structures are significant for only the (111) and (002) planes. With the exception of the intensities of these two planes, the observed values

were in general agreement with those calculated for both structures. The calculated and experimental data for these two planes are compared in Table III.

TABLE III Calculated and Observed Itensities for the (111) and (002) planes of  $Nd_4O_3C$ 

Structure Type	<u>Plane</u>	
	(111)	(002)
ZnS	100.0	33.2
<sup>Nd</sup> 1.00 <sup>0</sup> 0.79 <sup>C</sup> 0.24	100.0	66.4 ± 1.2*
NaCl	100.0	68.6

<sup>\*</sup> Standard Deviation of Measurement

On the basis of the data presented in this table, the oxycarbide is considered to possess a NaCl-type fcc structure having a lattice parameter  $a_0=5.1406\pm0.0007$  Å, where the error reported is the standard deviation of a least squares fit of the powder data.

Samples prepared using excess amounts of metal, oxygen, and carbon showed invariant lattice parameters, and indicate a narrow homogeneity range for this phase.

# 4. Hydrolysis Results

Graphic output of the vapor phase chromatograph displayed a very intense peak which was attributable to

methane, and a very weak peak which could be assigned to acetylene. The acetylene peak tailed off on the longer retention time side, displaying two small shoulders, presumably due to hydrolysis products similar to acetylene.

Planimeter measurements of the areas subtended by the two peaks, corrected for the difference in the flame-ionization detector response to methane and acetylene, indicated that the hydrolysis products consisted of  $96 \pm 3\%$  methane and  $4 \pm 2\%$  of a gas mixture of which acetylene comprised the major part.

An attempt was made to determine the conductivity of the  $Nd_4O_3C$  in a qualitative manner, by use of the pressed pellet technique. The conductivity appeared equivalent to that of an ingot of Nd metal of comparable size.

# D. Discussion, $Ln_4O_3C$ Phase

This ternary oxycarbide phase appears to be a carbon stabilized lanthanide monoxide. The apparently fixed C/O ratio is markedly different from the variable ratios exhibited by the previously discussed  $\text{ZrO}_{1-\epsilon} \overset{C}{\epsilon}^{31}$ and  $UO_{1-x}C_x^{10,14}$  phases which might be considered analogous to this  $Nd_4O_3C$  system. Fixed O/C ratios have been observed in the Ln<sub>2</sub>O<sub>2</sub>C<sub>2</sub> phases discussed previously. In these  $\operatorname{Ln_2O_2C_2}$  phases, the fixed O/C ratio was postulated to result from ordered anisotropic anion sites in the lattice, occupied by acetylide ions. These sites were considered different from the other spherical anion lattice sites which were occupied by oxide ions. This argument does not seem applicable in the  $Nd_{11}O_{3}C$  case, since the carbon units appear to be spherical methanide entities (discussed in the following section), and no evidence was found by x-ray diffraction for their ordering in the crystal. If the methanide units are indeed statistically distributed over the available anion sites, the C/O ratios might be varied over at least a moderate range, paralleling the behavior of the  $Ce(0,N)^{32,33,40}$  and the Sm(O,N) systems. 41 (This analogy between nitride, carbide and oxide ions is based on the fact that they form an isoelectronic series.)

A definitive explanation does not exist, therefore, for the apparently anomalously invariant C/O ratios found in this phase, but a number of postulates can be made whose consequences appear consistent with observed facts. If one examines the binary ionic compounds of the tripositive lanthanides formed with the anions of the isoelectronic series C<sup>-4</sup>, N<sup>-3</sup>, and O<sup>-2</sup>, he sees that the only stable 1:1 solid phase is that of LnN, as neither the LnC nor the LnO phase has been characterized. (Reports of solid LnO phases will be discussed subsequently.) This stability of the LnN can be postulated as being principally due to two factors:

- 1. Optimum anion radius
- 2. Apparent formal charge neutrality. Consequently, it can be postulated that the stability of any solid phase of a tripositive lanthanide with any combination of the isoelectronic series  $0^{-2}$ ,  $N^{-3}$ ,  $C^{-4}$  will be a maximum when both the formal charge neutrality and the average anionic radius approach that of the corresponding lanthanide nitride.

This postulate is supported by the  $Nd_4O_3C$  phase. The lattice parameter for this phase is  $a_0 = 5.1406 \pm 0.0007$  Å, which compares very favorably with the lattice parameter of NdN,  $a_0 = 5.151$  Å.  $^{29}$ 

The effective anionic radius in the phase  ${\rm Nd_4O_3C}$  calculated by the method described in Appendix VII, is

$$r_{eff} = .75(1.40) + .25(2.60)$$

$$r_{eff} = 1.70 \text{ Å}$$

based on the Pauling radii for  $0^{=}$  = 1.40 Å and  $C^{-4}$  = 2.60 Å. This calculated  $r_{\rm eff}$  compares favorably with the Pauling radius for  $N^{-3}$  = 1.71 Å.<sup>42</sup>

The formal charge on the neodymium in  $Nd_4O_3C$  is 2.5 rather than 3, so the second of the factors is not completely satisfied. In this case, however, the two criteria cannot be satisfied simultaneously, since the stoichiometry demanded for formal charge neutrality,  $Nd_2OC$  would possess an effective radius

$$^{\mathbf{r}}$$
eff = .5(.40) + .5(2.60) = 2.00 Å.

which is much larger than that required by the first criterion. Thus, in the Nd<sub>4</sub>O<sub>3</sub>C phase, at least, the requirement of formal charge neutrality is apparently the less stringent of the two factors. This is not inconsistent with the fact that many crystalline carbides of the lanthanides possess conduction bands which accept electrons from the lanthanide species, thereby producing a low oxidation state for the metal.

This general postulate has a number of other implications which will be discussed in the chapter describing future research.

There are several possibilities for placement of the methanide ions in the crystal lattice. They may be situated either as  $(a)C^{-4}$  methanide ions occupying one fourth of the octahedral anion sites, (b) randomly oriented  $C_2^{-2}$  acetylide units which occupy one eighth of the octahedral sites (and thereby leave one eighth of the anion sites vacant) or (c) a combination of the two.

Since the hydrolysis products consist almost entirely of methane, with only a trace of acetylene and its analogues, the carbon units appear to be present as the methanide ions. Even though the hydrolysis was effected principally by water vapor, some minor reaction of methanide ion to form acetylene, followed by subsequent reduction to more highly hydrated species cannot be precluded. In addition, the complete absence of trace amounts of a dicarbide impurity cannot be proven, but most of the carbon present must be considered to be in the form of methanide ions. Thus the second, and for the most part the third alternative schemes for carbon placement in the lattice may be eliminated. The hypothesis of methanide ions is not inconsistent with the x-ray diffraction results. That the cubic form appears to be

crystallographically stable at both room and elevated temperatures and not just a quenched, high temperature modification substantiates further this hypothesis, since acetylide-containing carbides usually exhibit symmetry different from cubic at room temperature due to the presence of the anisotropic acetylide species. 43

Furthermore, if the carbon were to exist in this phase in the form of acetylide ions, the formal oxidation state of the metal would be 1.75, compared with the value of 2.5 based on the methanide assumption. The higher formal oxidation value seems the more likely.

It seems desirable to compare the  ${\rm Ln_4O_3C}$  phase with the various reported lanthanon monoxides. The best characterized monoxide, EuO, is not strictly comparable, because of the much greater stability of the dipositive europium compared with that of the dipositive neodymium. The nitride-stabilized samarium monoxide is probably the best characterized "monoxide" if EuO is excluded. The smallest lattice parameter reported for the SmO  $(a_0=4.978\text{\AA})^{44}$  presumably describes the lattice of a sample least affected by nitride ion contamination. The difference between this parameter and that of  ${\rm Nd_4O_3C}$  is 0.162 Å. This difference can be accounted for in a relatively straight-forward

manner. To twice the increase in the ionic radius from  $\rm Sm^{+3}$  to  $\rm Nd^{+3}(0.031~\mathring{A})^{34}$  must be added the increase of the effective anion diameter over that of oxygen (2.80  $^{\circ}$ A)  $^{42}$ due to the presence of the larger methanide ions which occupy one fourth of the sites. This increase (c.f. p. 104) is 0.30 Å, and the calculated difference in the lattice parameter is 0.33. On the other hand, if one uses a methanide radius determined to be one fourth of the unit cell face diagonal of the methanide-type antifluorite phase Be<sub>2</sub>C,<sup>29</sup> corrected for the change in coordination from eight in the antifluorite to six in the NaCl structure by use of Pauling's formulation with an approximated Born exponent of 9,42 the increase in the effective anion radius is 0.06 Å, and the calculated difference in the lattice parameter for the SmO and  $Nd_4O_7C$  is 0.12 Å. The measured difference of 0.16 Å is bracketed by the two calculated values, but is somewhat close to the latter. It appears from the difference in the methanide ionic radii in the two computations that this ion is probably somewhat diffuse and readily distorted. It does appear, however, that the two phases are similar, the "samarium monoxide" being stabilized by nitrogen, thereby forming an oxynitride and the "neodymium monoxide" being stabilized by carbon, forming an oxycarbide. On the basis of the proposed postulate concerning phases of this type, the oxynitride should become less and less stable with a decrease in the  $N^{-3}/0^{=}$  ratio. Evidence of this behavior is demonstrated by the reported inability to prepare the samarium monoxide in the complete absence of nitrogen. 45

On the basis of this work, any "monoxide" except possibly EuO prepared by reduction of the sesquioxide with graphite might in truth be an oxycarbide. Additionally, the postulates deduced from this work imply that many of the other "monoxides" prepared by methods other than carbon reduction are oxynitrides, having variable O/N ratios.

The high conductivity of the  $\mathrm{Nd}_4\mathrm{O}_3\mathrm{C}$  phase is similar to that observed in most lanthanide carbide phases, leading to the assumption that the bonding is similar to that postulated for the carbides. Assuming this hypothesis to be true, the metal ion should be in a tripositive oxidation state and should supply electrons into conduction bands. The lattice parameter observed for the  $\mathrm{Nd}_4\mathrm{O}_3\mathrm{C}$  is

consistent with the existence of  $Nd^{+3}$  ionic units in the cell, as is demonstrated by the comparison of its observed lattice parameter with that of NdN, in which the  $Nd^{+3}$  unit has been established quite conclusively.

In this oxide carbide phase, each neodymium ion presumably could donate one half an electron to a conduction band (assuming all carbon units to exist as  $C^{-4}$  ions in the stoichiometry  $Nd_4O_3C$ ). Indeed, the silver-grey color of the phase is indicative of band occupation, but further conduction and magnetic studies are needed before definite statements can be made concerning the bonding.

#### CHAPTER IV. FUTURE RESEARCH

# A. $Ln_2O_2C_2$ PHASE

Two areas of great importance, structure and bonding, have yet to be investigated.

#### 1. Structure Determination

The structure determination is dependent on the possession of a small high quality single crystal of the  ${\rm Ln_2O_2C_2}$ . Some single crystals of uncertain quality were separated from the ingot of an arc melt, and some from the fused crust of the  ${\rm Ln_2O_2C_2}$ ,  ${\rm Ln_2O_3}$  and graphite equilibrium mixture. These crystals were the basis for some preliminary experiments as detailed further in Appendix III.

The vapor-phase transport method might also be used. In equilibration attempts with the Nd<sub>4</sub>O<sub>3</sub>C phase, small crystals were found growing on the underside of the crucible lid. Most of these crystals showed the gold color typical of the dicarbide, but toward the axial center of the crucible lid, some silver grey crystals were observed. These grey crystals were too small to permit any x-ray diffraction examination, but showed hydrolytic behavior typical of an oxycarbide upon exposure to atmospheric moisture. If, as it appears, this reaction can be described by the equation

$$LnO(g) + C(s) \rightarrow Ln(0,C)$$
 (s), (36)

oxycarbide crystals can be grown by passing LnO gas over a graphite surface whose temperature varies. (A carbon monoxide atmosphere has to be maintained in such a system to prevent decomposition of the oxycarbide.) Presumably oxycarbide crystals would be formed at that point on the graphite surface where the temperature was such that an equilibrium was maintained between the crystals formed and the carbon monoxide atmosphere. With suitable crystals such typical single crystal x-ray methods as the Weissenberg or precession method could be employed.

## 2. Bonding Studies

Studies into the fundamental nature of the bonding are, like the structure determination, dependent on pure crystalline samples. If such samples can be made, information concerning the oxidation state and resultant bonding of the oxycarbides could be collected by classical magnetic susceptibility and conductivity measurements.

# B. Ln<sub>4</sub>0<sub>3</sub>C PHASE

### 1. Structure and Bonding

The investigations outlined in the previous section for the  ${\rm Ln_2O_2C_2}$  phase are applicable here also. The molybdenum bomb which was described in Chapter III might be the best method for growing suitable crystalline material.

## 2. Thermodynamic Studies

Thermodynamic information about this phase might be accessible either by static or flow techniques. Preliminary experiments indicated a much lower equilibrium carbon monoxide pressure than that observed for the  $\rm Ln_2O_2C_2$  phase, thus a flow technique might be the preferred method.

# 3. Phases Based on Model Proposed in Chapter III, part D.

In the discussion section in Chapter III, a proposal was made that the cubic phases composed of lanthanide ions and anions of the isoelectronic series  $C^{-4}$ ,  $N^{-3}$ ,  $O^{-2}$  were most stable when the "effective anionic radius" approached that of the  $N^{-3}$  ion and charge neutrality was maintained. This proposal was used to explain why Ln(O,N) phases showed varying N/O ratios, becoming more stable as the N/O ratio increased; and why the  $Ln_4O_3C$  showed very narrow composition limits.

It would be of interest to extend this proposal to include F<sup>-</sup>, another member of the isoelectronic series. Such a substitution would suggest that a cubic oxyfluoride phase would have a variable O/F ratio, and that its stability would increase as the oxide anion concentration increased.

Another proposed phase would be Ln(C,F), a lanthanide carbide fluoride. Since one of the anions is larger and the other smaller than the  $N^{-3}$  ion, the proposed model would suggest that a fixed C/F ratio would be found, with the ratio such that the "effective anionic radius" would be equivalent to that of the  $N^{-3}$  ion. A proposed preparation method is described by the reaction

$$Ln(s) + CF(s) \rightarrow Ln(CF)$$
,

where the solid reactants are melted together, either in the arc melter or a suitable container such as platinum bomb.

Note: The graphite fluoride is thought to be ideally  $(CF)_n$ , and has been prepared with C:F ratios up to 1:0.99, and is a white, non-conducting solid.

#### CHAPTER V. BIBLIOGRAPHY

- 1. B. R. Geijer, Crell Ann., I. 229 (1788).
- 2. R. C. Vickery, Chemistry of the Lanthanons, Academic Press, N. Y., 1953.
- 3. O. Pettersson, Bericht., 28, 2419 (1895).
- 4. H. Moissan, Compt. Rend., 123, 148 (1896).
- 5. <u>Ibid.</u>, 131, 595 (1900).
- 6. H. Moissan, A. Etard, Compt. Rend., 122, 573 (1896).
- 7. G. L. Buchel, Thesis, Michigan State University (1963).
- 8. O. Heusler, Z. Anorg. u. Allgem. Chem., 154, 353 (1926).
- 9. J. R. Piazza, M. J. Sinnott, <u>J. Chem. Eng. Data</u>, <u>7</u>, 451 (1962).
- 10. R. F. Stoops, J. V. Hamme, <u>J. Am. Ceram. Soc.</u>, <u>47</u>, 59 (1964).
- 11. A. Heiss, M. Dode, Rev. Hautes Temp. Refract., 3, 245 (1966).
- 12. L. M. Litz, A. B. Garrett, F. C. Croxton, <u>J. Am. Chem. Soc.</u>, <u>70</u>, 1718 (1948).
- 13. M. W. Mallett, A. F. Gerds, D. A. Vaughan, <u>J. Electrochem.</u> Soc., <u>98</u>, 505 (1951).
- 14. P. Chiotti, W. C. Robinson, M. Kanno, <u>J. Less-Common Metals</u>, <u>10</u>, 273 (1966).
- 15. P. L. Blum, J. P. Morlevat, <u>Rev. Hautes Temp. Refract.</u>, <u>3</u>, 253 (1966).

- 16. E. K. Storms, Thermodynamics, 1, International Atomic Energy Agency, Vienna (1966) p. 309.
- 17. W. A. Chupka, J. Berkowitz, C. F. Giese, M. G. Inghram, J. Phys. Chem., 62, 611 (1958).
- 18. F. H. Spedding, K. Gschneider, A. H. Daane, <u>J. Am. Chem. Soc.</u>, <u>80</u>, 4499 (1958).
- 19. I. M. Klotz, W. A. Benjamin, Chemical Thermodynamics, N. Y., (1961).
- 20. C. N. Lewis, B. Randall, <u>Thermodynamics</u>, 2nd edition, revised by K. S. Pitzer, L. Brewer, McGraw-Hill, New York, N. Y. (1961).
- 21. A. Findlay, The Phase Rule, ninth edition, revised by F. N. Campbell, N. O. Smith, Dover, N. Y. (1951).
- 22. A. D. Butherus, R. B. Leonard, G. L. Buchel, H. A. Eick, <u>Inorg. Chem.</u>, 5, 1567 (1966).
- 23. E. J. Huber, C. E. Holley, Jr., <u>J. Am. Chem. Soc.</u>, <u>75</u>, 3594 (1953).
- 24. F. D. Rossini, D. D. Wagman, W. H. Evans, S. Levine, K. Jaffe, U. S. National Bureau of Standards Circular 500, Series I, U. S. Government Printing Office, Washington, D. C., 1952, p. 99.
- 25. R. C. Vickery, R. Sedlacek, A. Ruben, <u>J. Chem. Soc.</u>, 503 (1959).
- 26. G. J. Palenik, J. G. Warf, <u>Inorg. Chem.</u>, <u>1</u>, 345 (1962).
- 27. M. J. Bradley, L. M. Ferris, <u>Inorg. Chem.</u>, <u>1</u>, 683 (1962).
- 28. M. Atoji, <u>J. Chem. Phys.</u>, 35, 1950 (1961).

- 29. A. Taylor, B. J. Kagle, <u>Crystallographic Data on Metal</u> and Alloy Structures, Dover, New York, N.Y., (1963).
- 30. F. Leprince-Ringuet, Compt. Rend., 264, 1957 (1967).
- 31. F. Leprince-Ringuet, A. Lejus, R. Collongues, Compt. Rend., 258, 221 (1964).
- 32. H. A. Eick, K. Manske, Report at American Chemical Society Convention, Miami Beach, Florida, April, 1967.
- 33. H. A. Eick, N. C. Baenziger, L. Eyring, <u>J. Am. Chem.</u> Soc., <u>78</u>, 5147 (1956).
- 34. D. H. Templeton, C. H. Dauben, <u>J. Amer. Chem. Soc.</u>, <u>76</u>, 5237 (1954).
- 35. J. O'M Bockris, J. L. White, J. D. McKenzie,

  Physioco-chemical Measurements at High Temperatures,

  Academic Press, N. Y. (1959).
- 36. Handbook of Chemistry and Physics, Edition 48, p. E-164, Cleveland (1967).
- 37. J. N. Gregory, D. Mapper, Analyst, 80, 225 (1955).
- 38. H. A. Sloman, C. A. Harvey, O. Kubaschewski, J. Inst. Metals, 80, 391 (1951-2).
- 39. D. T. Cromer, J. T. Waber, Acta. Cryst., 18, 104 (1965).
- 40. H. A. Eick, unpublished work.
- 41. H. A. Eick, "Rare Earth Borides and Nitrides,"
  Rare Earth Research, E. V. Kleber, Ed., The
  Macmillan Co., New York, (1961).
- 42. L. Pauling, The Nature of the Chemical Bond, p. 514, Third ed., Cornell Univ. Press, Ithaca (1960).

- 43. A. L. Bowman, N. H. Krikorian, O. P. Arnold, T. E. Wallace, N. G. Neverson, Presented at 6th Rare Earth Conf., Gatlinburg, Tenn., May 1967.
- 44. L. Eyring, Private communication.
- 45. W. Klemm, G. Winkleman, Z. Anorg. u Allgem. Chem., 288, 87 (1956).

#### CHAPTER VI. APPENDICES

### APPENDIX I. SOURCES AND PURITY OF MATERIALS

- La Metal, 99% Purity, Research Chemicals, Div. of Nuclear Corp. of America, Box 14588, Phoenix, Arizona.
- 2. Nd Metal, 99% Purity, Michigan Chemical Co., St. Louis, Mich.
- 3. La<sub>2</sub>O<sub>3</sub> 99.9+% Purity, Research Chemicals, Div. of Nuclear Corp. of America, Box 14588, Phoenix, Arizona.
- 4. Nd<sub>2</sub>0<sub>3</sub>, 99.9% Purity, Michigan Chemical Co., St. Louis, Mich.
- 5. Graphite, No. 38 Powder, Fisher Scientific Co., 1 Reagent Lane, Fair Lawn, N.J.

# APPENDIX II. HIGH SPEED PUMPING SYSTEM AND CURRENT CONCENTRATOR

The pumping system used (Fig. 7) consists of a Cenco Hyvac No. 45 mechanical pump (Central Scientific Co., 2600 Kostner Ave., Chicago, Ill.) backing a four inch oil diffusion pump (Consolidated Vacuum Co., Rochester 3, N.Y.) and a four inch, baffled liquid nitrogen cold trap.

The heating portion of the system was enclosed in a 35 cm long 100 mm ID Pyrex pipe, which sat on a flat silicone rubber gasket in a flanged fitting which lead to the pumping system. The current concentrator hung from a flat, water-cooled lid, which was attached by a similar gasket to the base flange. The heating system was sealed by atmospheric pressure on both flat gaskets.

The water-cooled current concentrator consists of a copper donut which acts similarly to the core of a transformer and forces the toroidally-shaped field to pass through the hole in the donut. Such a shaping of the field causes it to couple very efficiently with the crucible.

The entire concentrator was prevented from coupling to the induction field by a vertical cut which prevented establishment of a closed conduction loop in the copper.

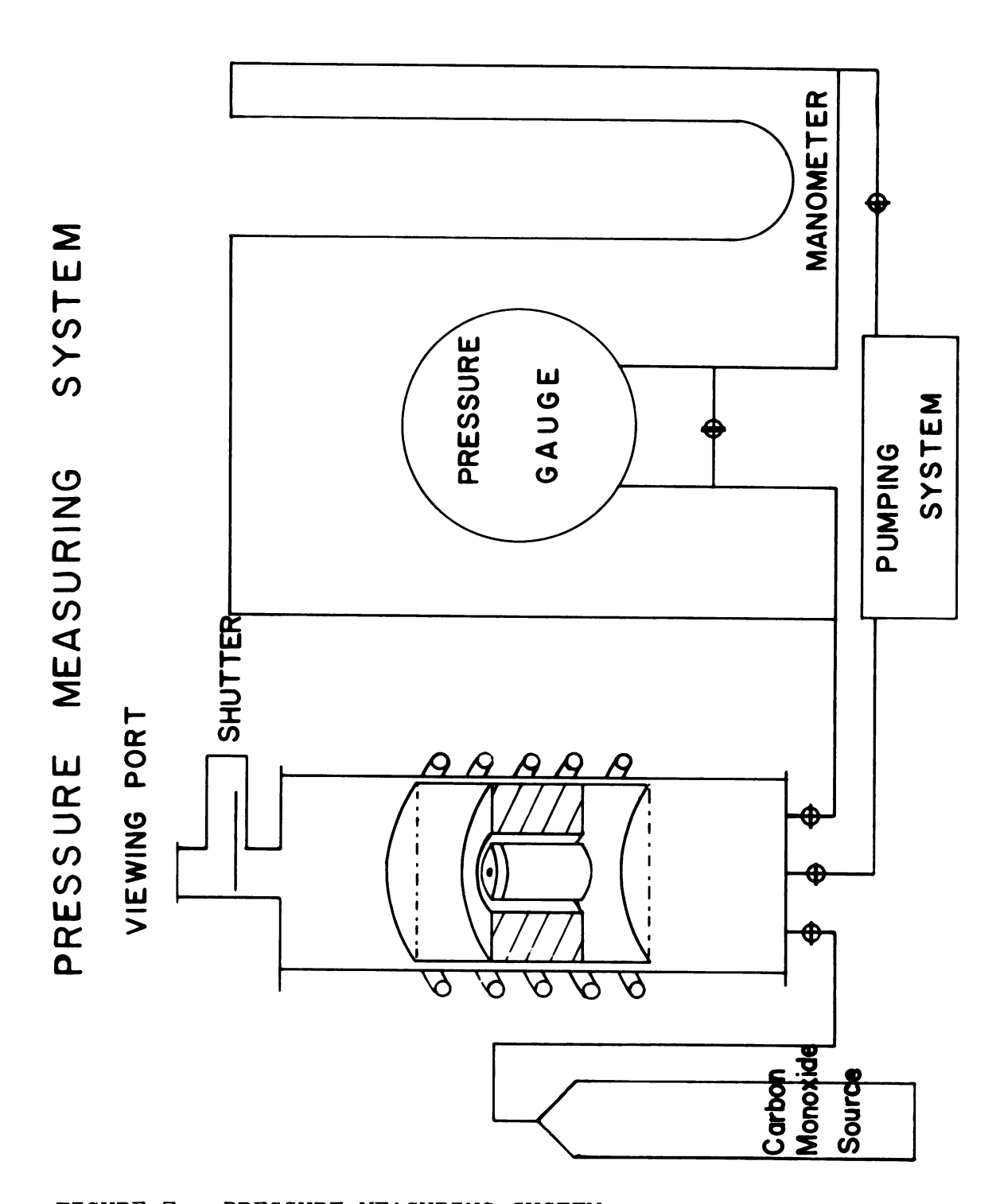


FIGURE 7. PRESSURE MEASURING SYSTEM

# APPENDIX III. TENTATIVE INDEXING OF La202C2

Based on Weissenberg X-ray studies of a poorquality single crystal of  $\text{La}_2\text{O}_2\text{C}_2$ , a monoclinic unit cell was proposed and all possible d-values from that proposed cell were calculated and compared with the observed Some modification of the proposed cell proved to be necessary, since some of the axes used in the Weissenberg studies were apparently not principal axes. parameters of the proposed monoclinic unit cell for La<sub>2</sub>0<sub>2</sub>C<sub>2</sub> are:

 $a = 7.289 \stackrel{\circ}{A}$   $b = 3.529 \stackrel{\circ}{A}$ 

c = 7.028 Å

 $\beta = 84.37^{\circ}$ 

#### APPENDIX IV. ARC ZONE MELTER

The arc zone melter (Figure 8) consists of an assembly that is fastened to the hearth of the arc melter previously described (Figure 1). The electrode was mechanically attached to a traveling block, which was driven horizontally by an electrically-driven lead screw. The arc traversed a 10 cm long groove milled in the hearth. The samples were pelletized, laid in the hearth groove and then arced. The electrode could be driven at various speeds.

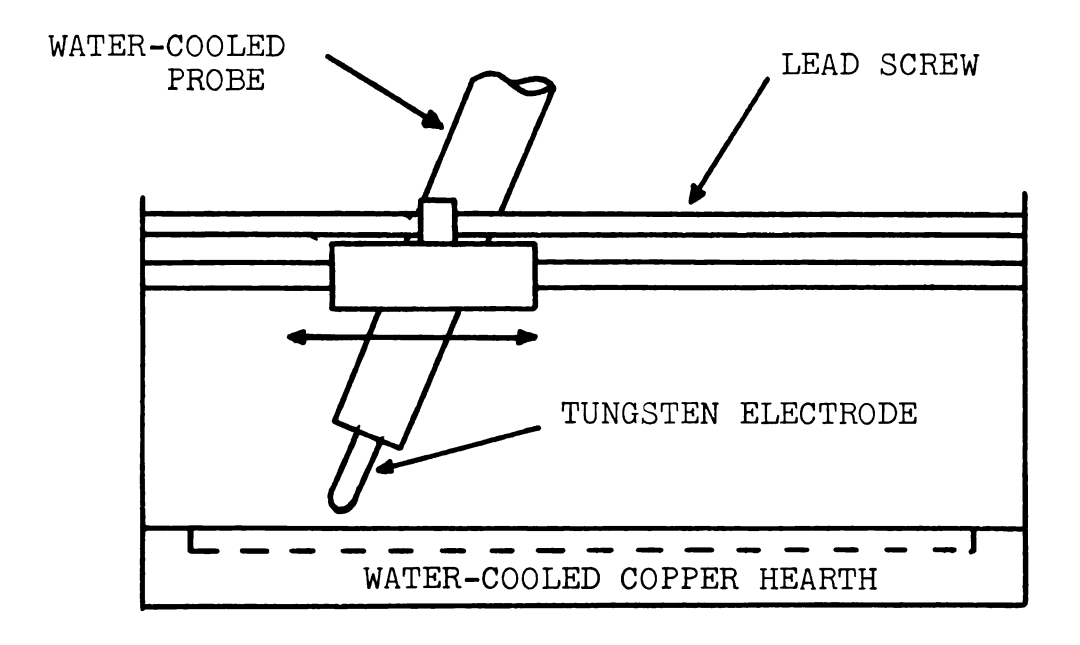


FIGURE 8, ARC ZONE MELTER

.

The So

#### APPENDIX V. ELECTRON BEAM ZONE MELTER

The Model EZB-94 zone melter (c.f. page 84) consists of a vacuum chamber and pumping system in which was placed the mechanical drive mechanism and separate from this assembly, a high potential DC power supply (Figure 9).

The sample was mounted vertically inside the vertical traverse of a circular thoriated tungsten filament, which could be driven mechanically at speeds as low as 1 mm per hour.

After the chamber had been evacuated by the pumping system, the filament was heated and a milliamp-range current was induced to flow from the filament to the sample by a potential in the 15 to 50 kilovolt range. The electrons boiled off the filament were accelerated by this high potential and transferred this energy to the sample upon collision. This technique heated a rather flat cross section of the sample. This heated zone was swept down the sample by the mechanical drive.

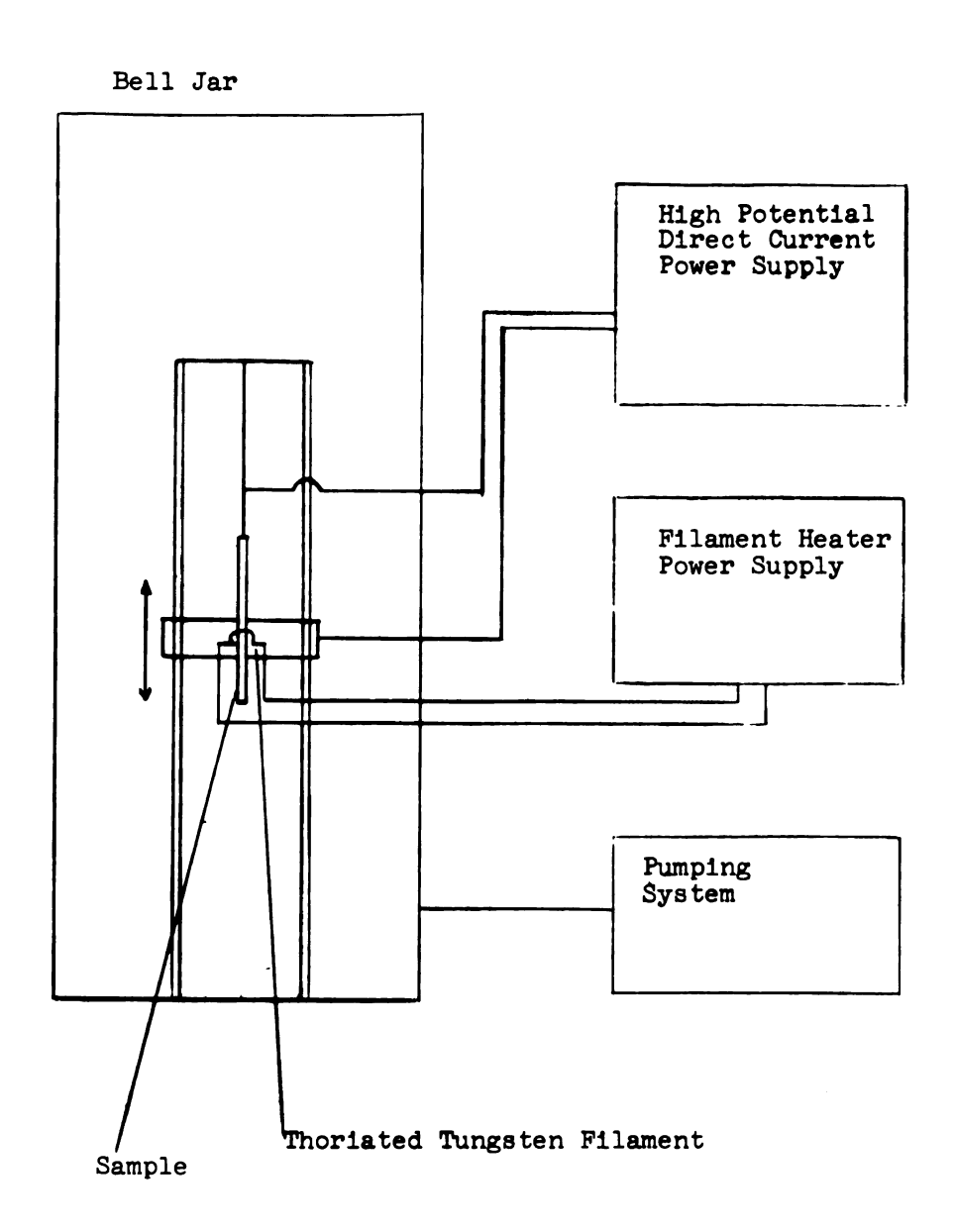


Figure 9. Electron-Beam Zone Melter.

APPENDIX VI. CALCULATED INTENSITIES FOR X-RAY POWDER DIFFRACTION LINES OF  $\text{Nd}_4\text{O}_3\text{C}$  IN ZnS and NaCl LATTICE TYPES

(h,K,l)	Relative Itensity Calculated	
	NaCl Lattice	ZnS Lattice
111	100.0	100.0
002	68.6	33.2
022	8.8	6.7
113	16.7	15.5
222	6.8	3.7
004	2.8	2.1
133	5.0	4.5
024	5.8	3.4
224	3 <b>.</b> 6	2.8
333, 115	2.2	1.9
004	1.0	0.7
135	1.7	1.5
244 <b>, 0</b> 06	0.1	0.1

#### APPENDIX VII. EFFECTIVE ANIONIC RADII

In solid phases which contain two or more types of anion, two possibilities exist for the distribution of the anion sites. They may be regularly situated so as to form a super lattice of some type, or may be statistically distributed.

In the first case, such behavior can usually be detected in the x-ray diffraction patterns. In the second case, no extraneous lines appear in the x-ray diffraction pattern, though the line intensities sometimes are different from what one would anticipate from either anion singly occupying the lattice sites. This is due to the differences in scattering of the x-rays by the two anions.

In the statistically-distributed anion case, we define the effective anionic radius to be a linear combination of the two separate radii. This procedure yields a composite radius with the contribution of each anion proportional to the fraction of anionic sites it occupies.

For example, in the general case for a phase  $$^{\mbox{\scriptsize MX}}_{a}\mbox{\scriptsize Y}_{b}$$ 

with the anions statistically distributed in the lattice, the effect anionic radius  $\mathbf{r}_{eff}$  would be the linear combination of the two anionic radii  $\mathbf{r}_{x}$  and  $\mathbf{r}_{y}$ .

$$r_{eff} = \frac{a}{a+b} r_x + \frac{b}{a+b} r_y$$

